12-2020

Infiltration and Inflow as a Component of the Urban Water Cycle: Inter-Watershed Comparison of Magnitude and Correlative Watershed Attributes

Allison D. Murray

INFILTRATION AND INFLOW AS A COMPONENT OF THE URBAN WATER CYCLE: INTER-WATERSHED COMPARISON OF MAGNITUDE AND CORRELATIVE WATERSHED ATTRIBUTES

by

ALLISON DIAMOND MURRAY

Under the Direction of Luke Pangle, PhD

ABSTRACT

Infrastructure-mediated flows (IMFs), such as infiltration and inflow (I&I) of precipitation and groundwater into sanitary sewer systems are difficult to measure and complicate the calculation of urban water budgets. Available I&I quantification methods are based on broad assumptions and do not fully exploit the information content of sensor networks and databases commonly administered by watershed management agencies. This study includes detailed calculations of I&I within 14 tributary basins of the South River Watershed, which has its headwaters in the southeastern portion of the Atlanta Metropolitan Region, USA. The analysis leverages a network of approximately 200 flow meters installed within the sanitary pipes maintained by the DeKalb County Department of Watershed Management. Results revealed little correlation between I&I and watershed attributes, indicating spatial variability which eliminates watershed attributes as indicators of I&I. It is therefore paramount for water managers to use system wide monitoring programs to mitigate the effects of I&I.

INDEX WORDS: Infiltration and inflow (I&I), Urban hydrology, Infrastructure-mediated flows (IMFs), Sanitary sewer overflow (SSO), South River

INFILTRATION AND INFLOW AS A COMPONENT OF THE URBAN WATER CYCLE: INTER-WATERSHED COMPARISON OF MAGNITUDE AND CORRELATIVE WATERSHED ATTRIBUTES

by

ALLISON DIAMOND MURRAY

A Thesis Submitted in Partial Fulfillment of the Requirements for the Degree of

Master of Science

in the College of Arts and Sciences

Georgia State University

2020

INFILTRATION AND INFLOW AS A COMPONENT OF THE URBAN WATER CYCLE: INTER-WATERSHED COMPARISON OF MAGNITUDE AND CORRELATIVE WATERSHED ATTRIBUTES

by

ALLISON ROSE DIAMOND

Committee Chair: Luke Pangle

Committee: Sarah Ledford

Richard Milligan

Electronic Version Approved:

Office of Graduate Studies

College of Arts and Sciences

Georgia State University

December 2020

DEDICATION

I dedicate this thesis to my parents, Mark and Shay Diamond, for giving me the courage to chase my dreams and the tools to achieve them, and to my husband, Allen Davis Murray, for filling my life with love and renewed purpose.

ACKNOWLEDGEMENTS

First and foremost, I thank my advisor, Dr. Luke Pangle, for helping me navigate graduate school and for the hours he spent assisting me with this thesis. I also acknowledge my other committee members, Dr. Sarah Ledford and Dr. Richard Milligan, for their numerous contributions to the development of this thesis and my academic/ professional growth. My peers and colleagues, especially Faustina Jones and Hannah Knab, played an important role in helping me with GIS and preparing me for my defense; thank you, friends. This thesis would not be possible without the efforts of my family, who fed, housed, encouraged, and loved me throughout my academic journey. A special acknowledgment to my husband for always encouraging me to continue my education, even when it meant living apart.

TABLE OF CONTENTS

LIST OF TABLES

LIST OF FIGURES

LIST OF ABBREVIATIONS

List of Abbreviations

ACF	Autocorrelation Function
AR	Auto-regressive
ARMA	Auto-regressive moving-average
CSO	Combined sewer overflow
D	Water distributed into the basin through infrastructure for municipal supply
D_{loss}	Water distribution lost from the basin
D_S	Municipal water distributed
DWM	DeKalb County Department of Watershed Management
EPA	Environmental Protection Agency
ET	Evapotranspiration
I&I	Inflow and Infiltration
IBT	Interbasin Transfer
IMF	Infrastructure-mediated flow
MA	Moving-average
ORR	Open Records Request
P	Precipitation
$Q_{I\&I}$	Meteoric (rainfall-derived) infiltration and inflow into sanitary sewer systems
Q_L	Runoff and groundwater discharge
Q_R	River discharge
Q_{WWTP}	Effluent from upstream wastewater treatment plants
SRW	South River Watershed
SSO	Sanitary sewer overflow
SSS	Sanitary sewer system
WWTP	Wastewater treatment plant

1 INTRODUCTION

Water infrastructure has historically been an agent of immense social and environmental change. If water infrastructure is well-planned, efficient, and universally accessible, a city benefits from economic growth, human and ecological wellness, fire protection, and greater human rights. Conversely, a city with poor water infrastructure may suffer from pollution, illness, inequity, inequality, fire, water shortages, and more (Borden, 2014). Under the modern confluence of urbanization, climate change, and population growth, water infrastructure will continue to shape social and environmental change.

1.1 Water infrastructure

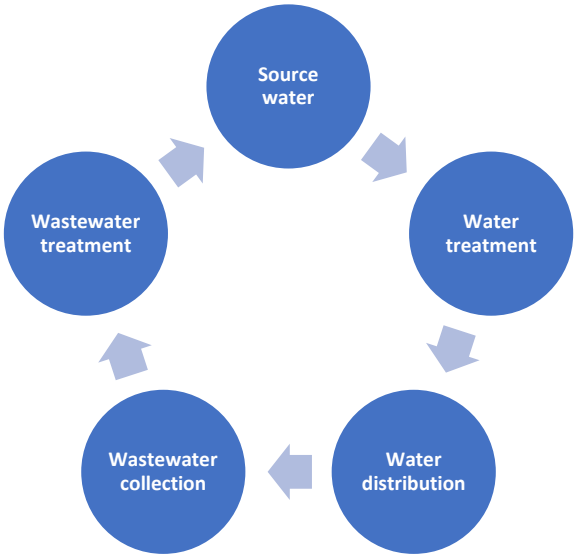

Figure 1.1 Movement of water through a typical municipality: (1) Source water and stormwater; (2) water treatment; (3) water distribution; (4) wastewater collection; (5) wastewater treatment.

Municipal water infrastructure functions in six steps (BC Water & Waste Association, 2020). First, water is sourced from surface or groundwater. Then, it is treated until suitable for human use. Potable water is distributed through pipes to consumers. The fourth step is

wastewater collection via stormwater, sanitary, and/or combined sewer systems. Sanitary sewers transport human waste in wastewater from buildings directly to treatment centers, while stormwater sewers, with few exceptions, carry stormwater into streams. Combined sewers simultaneously carry the stormwater runoff and human waste. Finally, wastewater is treated in specialized facilities and discharged back into waterways (Drinan and Spellman, 2013).

Deterioration of water infrastructure is problematic because stressed pipes are likely to crack, burst, and overflow (Borden, 2014; EPA, 2014; Drinan and Spellman, 2013; Klepper, 2015; McWillians, 2012). Sewer decay is affected by age, material, length, construction period, use, shape, location, depth, size, and slope (Ana et al., 2009). The significance of each factor varies with location, which may explain conflicting conclusions about which is most important (Ana et al., 2009; Baur and Herz, 2002; Hyeon-Shik et al., 2006). Age is frequently considered a significant factor affecting the overall performance of sewer systems (Ana et al., 2009; Kesik, 2015; Thapa et al., 2019; Wittenberg and Aksoy, 2010) because, over time, the remaining useful life of pipes and sewer elements is diminished. Also, the original carrying capacity of a sewer system may be exceeded over time.

Sewer pipe material and manufacturing techniques additionally impact the rate of sewer deterioration. Different materials have unique lifespans, strengths, and weaknesses. For example, the lifespan of cast iron pipes depends on age because manufacturing techniques and materials evolved over time. Pipes installed during the late 1800s- early 1900s need to be replaced after 120 years, on average. The 1920s-era pipes are expected to last 100 years. Post-World War II pipes last about 75 years (AWWA, 2001; City of Tampa, 2020; Thapa et al., 2019). Other materials used throughout history include clay/ brick stoneware, wood, cast iron, steel, PVC, iron, and polymer concrete (Cooper, 2009; Oszczapińska, 2020).

Sewer overflows are generally caused by three conditions: capacity limitations, structural defects, and maintenance problems (DeKalb DWM, 2015b). Utilities sometimes mitigate peak flows through combined sewer systems caused by heavy rain by planning Combined Sewer Overflows (CSOs), which transport wastewater from the overwhelmed sewer pipes into designated pipes that drain into a ditch or waterway. Sanitary sewer overflows (SSOs) are unintentional and occur when raw sewage spills out of pipes and wastewater treatment facilities into waterways (Borden, 2014).

1.2 History of Urban Water Management in Atlanta, GA

The first wells in Atlanta, Georgia, were installed in 1843 to ease fire safety concerns. Atlantans' fear of fire increased when General Sherman burned down the city in 1864. A new city waterworks was built in the 1870s and provided additional fire protection via a reservoir, cast iron pipes, and 75 fire hydrants. In 1892, the city began pumping water from the Chattahoochee and built water mains, cast iron pipes caulked with molten lead, and a waterworks building. Many of these pipes are still in use today, and the Chattahoochee River remains Atlanta's drinking water source (Borden, 2014; Kaufman, 2007; Neumann et al., 2005).

The sewer pipes built prior to 1910 were primarily combined sewers (Kaufman, 2007). Crude sewage ditches collected human waste and began flooding Atlanta with disease-ridden filth and legendary stink. Poor living conditions in sizeable "slums" bred water-borne illness, prompting the city's death rate to rise 150% above the 1908 national average (Borden, 2014). In response, all sewers built after 1910 utilized separate sewer and stormwater piping (Kaufman, 2007). By the 1920s, only 20% of sewer and stormwater systems treated wastewater before discharging into waterways (Borden, 2014).

Figure 1.2 Photograph of construction on Atlanta Connally Sewer (WPA, 1936).

In the 1930s, President Roosevelt's Works Progress Administration funded new city sewer lines, expansion of existing lines, and new sewage treatment plants (Borden, 2014). Additional water mains were added in the 1940s to increase withdrawals from the Chattahoochee River. Suburban areas also began building their own water utilities (Borden, 2014). The subsequent surge in water and electricity demand was intensified by a World War II manufacturing boom (Gillespie, 2016).

The Buford Dam was built in the 1950s to stabilize the streamflow in the Chattahoochee River, thereby protecting Atlanta's drinking water supply and assisting in flood control (Borden, 2014; Gillespie, 2016). The dam also generates hydroelectricity, increases downstream navigability, and provides recreation opportunities (Borden, 2014; Gillespie, 2016). The dam enables the Chattahoochee River to remain the major water source and primary transporter of municipal wastes throughout Metro-Atlanta (Stamer et al., 1976).

Urbanization in the 1960s and 1970s created more water infrastructure challenges and larger demands on the Chattahoochee River (Borden, 2014; Stamer et al., 1976). To maintain rapid development, local utilities around Metro-Atlanta built water supply infrastructure before

wastewater facilities. For instance, in the 1960's, only 16 of the 50 public water systems in Metro-Atlanta had public sewer systems (Borden, 2014). Buried wastewater treatment tanks for single-home use, called septic tanks, supplanted sewer systems in approximately 70% of suburban homes. The lag time between building water supply and sewer systems is referred to as a "water-sewer time lag" (Borden, 2014). Separate septic systems, buried on-site wastewater treatment tanks for single-home use, were used in the absence of sewer systems. Around 70% of suburban homes used septic tanks in 1960 (Borden, 2014). Today, Gwinnett County reports that 30% of its residents use septic systems, making it one of the highest concentrations of septic systems in the United States (Gwinnett County, 2020). Septic tanks degrade water quality because seepage carries non-point source pollution into groundwater and streams (Anderson, 2010; Borden, 2014; Burns et al., 2005; Kaufman, 2007). Concomitantly, highway expansions and residential/ industrial developments increased imperviousness and accelerated runoff into streams and storm drains (Borden, 2014; Burns et al., 2005; Smucygz et al., 2010). Overloaded sewer systems triggered more CSOs and degraded water quality (Stamer et al., 1976).

A string of federal and state regulations, along with citizen groups, forced the city to "clean up" or face fines (Borden, 2014; Stamer et al., 1976; Kaufman, 2007). In 1972, the Federal Water Pollution Act of 1948 was amended and became widely known as the Clean Water Act (CWA). The CWA mandated a permitting system, called the National Pollutant Discharge Elimination System (NPDES), for point source pollution discharges into US waters and gave the EPA authority to enforce water quality standards. Metro-Atlanta municipalities were pushed by the Georgia Environmental Protection Division (EPD) to install more wastewater treatment plants, but sewer overflows continued. In 1986, the state expanded the MRPA's oversight

powers and made the ARC's recommendations more enforceable. The CWA was expanded the following year to require permits for stormwater discharges by 1994 (Borden, 2014).

The Georgia Environmental Protection Division once described the state's historic water management decisions as "largely in response to specific needs or issues" and articulated the need for proactive planning. The Georgia Comprehensive State-Wide Management Plan, passed in 2008, outlines a more long-term, proactive, and comprehensive policy approach to maintaining growth while protecting ecosystems and is supported by state statutes and rules (EPD, 2008). First, the state must measure its water resources consumption and determine its needs during a dry year. Second, the state must forecast future water resources demands. Third, the state must create a framework for regional water development and conservation plans.

Today, water quantity and quality management issues remain rampant throughout Metro-Atlanta. The American Society of Civil Engineers gave Georgia a 2019 Infrastructure Report Card Grade of just C+, citing "consistently underfunded" water utilities and "deficiencies in the condition and capacity" of water plants, pumping stations, and pipes (ASCE, 2019). This study investigates how one deficiency—namely, leaky sanitary-sewer infrastructure—has the potential to alter the hydrology of urban watersheds, reduce wastewater-management capacity, and enhance human exposure to sanitary-sewer overflows.

1.3 "Natural" vs. Urban Hydrologic Cycle

1.3.1 *"Natural" hydrologic cycle*

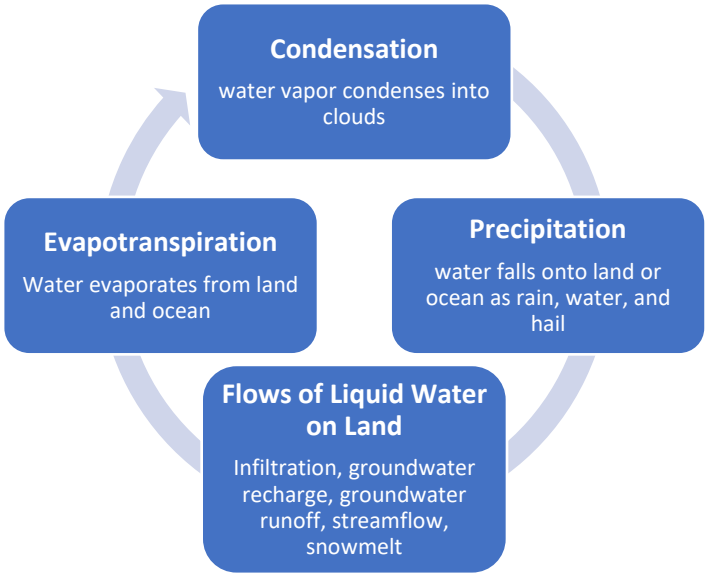

Figure 1.3 The Terrestrial Hydrologic Cycle

Our conception of the natural hydrologic cycle on land —in the absence of human perturbation—involves the condensation of atmospheric water vapor into precipitation that falls over land and ocean; the redistribution of this liquid water into surface-water bodies by overland flow; the slower infiltration of water into soils and aquifers, which ultimately discharge to surface-water bodies or oceans; and finally, the evaporation or transpiration (by plants) of liquid water from land and its turbulent transport back into the atmosphere. Each flow of water happens over different, and variable time scales, and involves markedly different magnitudes of water.

Invoking the principle of conservation of mass, the hydrologic cycle on land can be represented quantitatively as a closed budget. Change in the amount of water stored within a

watershed over some increment of time (dS/dt) is calculated by subtracting watershed outputs from inputs; assuming mass is conserved, the difference between input and output rates is equal to the rate of change of mass stored in the watershed. Considering a watershed that is geologically closed (i.e., not gaining or losing water due to groundwater inflow or outflow), the water budget can be written simply as below:

$$(1)\ \frac{dS}{dt}(t) = Inflows\ - Outflows = \ P(t) - ET(t) - Q(t)$$

where S is water storage in the watershed, P is precipitation rate [L^{3}-T^{-1}], ET is the combined flows of evaporation and transpiration [$L^{3}T^{-1}$], and Q is stream discharge [$L^{3}T^{-1}$].

1.3.2 *Urban hydrologic cycle*

The water cycle is different in urban watersheds, where land cover and land use are altered (Bhaskar et al., 2016a; Bhaskar et al., 2016b; Bhaskar and Welty, 2012; DeKalb DWM, 2015; Paul and Meyer, 2008; Rose and Peters, 2001; Walsh et al., 2005). Precipitation sometimes infiltrates into the water table but more frequently encounters impervious surfaces (roads, roofs, and paths) and becomes run-off. Run-off is funneled into pipes or surface streams. Surface and groundwater are withdrawn for human use, piped through water infrastructure, and discharged back into streams. Water is occasionally pumped from one watershed into another, typically for drinking water purposes; this is called an interbasin transfer (IBT). The literature is inconclusive in determining a dominant outflow in urban water balances, of which there are many more than just runoff (Bhaskar and Welty, 2012).

Impervious surfaces create a barrier between stormwater and soil, preventing infiltration and groundwater recharge while increasing runoff rates. Generally, urban areas manage increased runoff with stormwater drainage systems that efficiently transport stormwater to streams or WWTPs. This rerouting of stormwater may lead to decreased infiltration, which is

most pronounced when stormwater pipes drain directly into streams. In some cases, stormwater infiltration structures successfully mitigate increased runoff by increasing infiltration and groundwater recharge (Bhaskar et al., 2016a; Bhaskar et al., 2016b; Bonneau et al., 2017). In urban areas, "pervious" land coverings are often compacted during construction and have low infiltration capacities (Bhaskar et al., 2016a).

Underground pipes, including water supply and sewer networks, form "urban karst" (Bonneau et al., 2017). Like geologic karst, urban karst consists of subsurface cracks and permeable pockets that create flow paths and storage for infiltrated stormwater. In this case, however, the altered paths are created by infrastructure (Bonneau et al., 2017) and can contribute to groundwater recharge (Bhaskar and Welty, 2012). For example, gravel or sand usually surround buried pipes and form highly permeable pockets for potential groundwater storage. Trenches around gas or water supply pipes also create additional subsurface flow pathways. Additionally, water can escape leaky pipes and infiltrate into the soil (Bhaskar et al., 2016a; Bonneau et al., 2017); leakage increases with imperviousness because they both reflect degree of urbanization, however leakage is highly variable over space and time (Bhaskar and Welty, 2012).

Changes in land use and cover also impact the urban water budget. Decreases in vegetative land cover and increases in lawn irrigation (much of the water used for lawn irrigation becomes runoff) are both known to reduce evapotranspiration in urban watersheds. Also, impervious surfaces may indirectly increase precipitation due to the urban heat island effect (Bhaskar and Welty, 2012).

The urban water budget can be written as below:

$$(2)\ \frac{dS}{dt}(t) = inflows - outflows = P(t) + D(t) - ET(t) - D_{loss}(t) - Q_R(t)$$

where P is the precipitation rate [L^3T^{-1}], D is municipal water distribution [L^3], and ET is evapotranspiration [L^3T^{-1}] and Q_R is river discharge[L^3T^{-1}]. D_{loss} is a lumped term that refers to the portion of municipal water that does not return to streams or sanitary sewer systems [L^3T^{-1}], including: water collected by sanitary sewer systems that return to wastewater to a different watershed; municipal water used for irrigation or leaked from conveyance infrastructure; other mechanisms of export from a watershed (like the use of water in the production and distribution of beverages). River discharge can be further written as:

(3) $Q_R = Q_L + Q_{WWTP}$

where Q_L is runoff and groundwater discharge [L^3T^{-1}] and Q_{WWTP} is effluent from upstream wastewater plants [L^3T^{-1}]. Effluent from upstream wastewater plants (Q_{WWTP}) is expressed as:

(4) $Q_{WWTP} = D_S + Q_{I\&I}$

where D_S is municipal water distributed into a watershed [L^3T^{-1}] and $Q_{I\&I}$ is rainfall-induced infiltration and inflow into sanitary sewer systems[L^3T^{-1}]. Consolidating these equations, the complete urban water budget is:

(5) $\frac{dS}{dt}(t) = inflows - outflows = P(t) + D(t) - ET(t) - D_{loss}(t) - Q_L(t) - D_S(t) - Q_{I\&I}(t)$

1.3.3 *Key differences*

The natural and urban water budgets differ in both inputs and outputs. These variances indicate the presence of infrastructure-mediated flows (IMFs). Infrastructure-mediated flows are alterations in surface and groundwater flows caused by infrastructure which include but are not limited to the following: impervious surfaces, water supply pipes, sewer systems, wastewater treatment plants, and interbasin transfers.

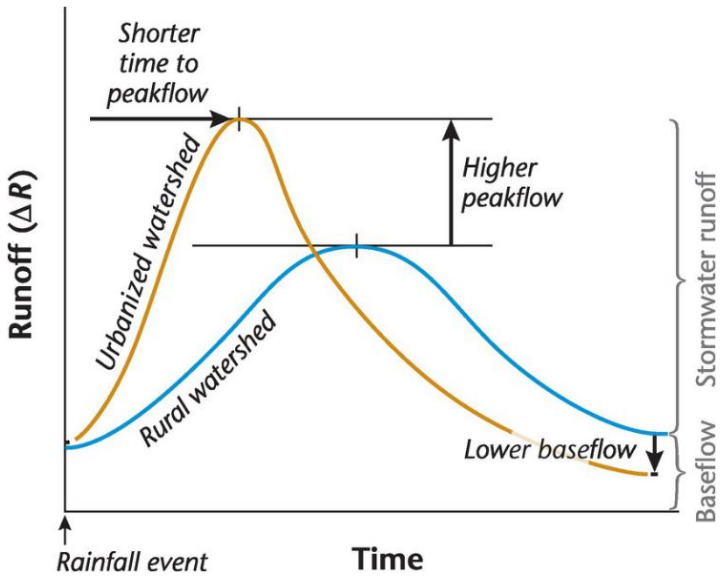

Figure 1.4 Example hydrograph of urbanized and rural watersheds (Oke, 2017)

Storm responses in urban and natural watersheds differ in several ways. First, urban storm events are marked by a decrease in time between precipitation and initiation of runoff peak flow (Bhaskar and Welty, 2012). This "flashy" response is most pronounced when stormwater sewers drain directly into streams (Bhaskar et al., 2016b). Second, urbanized watersheds have greater streamflow sensitivity than natural rural watersheds (Bhaskar and Welty, 2015). Studies show that urban baseflow response varies based on imperviousness, IBTs, stormwater management strategies, changes in evapotranspiration, and the effects of urban karst (Bhaskar et al., 2016a; Bhaskar et al., 2016b; Bhaskar and Welty, 2015). Urban baseflow response is sometimes marked by a non-pervasive decreased low flow from reduced groundwater recharge (Rose and Peters, 2001), and other times shows rising water tables and baseflow (Bhaskar et al., 2016a).

1.4 Infiltration and Inflow (I&I)

Wastewater has three main components: base sanitary (wastewater) flow, groundwater infiltration, and rainfall derived inflow. Base sanitary flow includes wastewater from domestic,

commercial, institutional, and industrial facilities. This study focuses on groundwater infiltration and rainfall derived inflow, which are collectively referred to as infiltration and inflow (I&I) (EPA, 2014; Kesik, 2015; Rodel, 2017).

1.4.1 *Sources of I&I and their hydrological and environmental impact*

Inflow is rainwater that directly or indirectly enters sewer pipes from above-ground sources like drains, manhole covers, and faulty plumbing connections. Infiltration is groundwater that unintentionally enters the sewer pipes from the ground via malfunctioning pipes, connections, maintenance holes, etc. (Belhadj et al., 1995; Cahoon and Hanke, 2017; De Bénédittis and Bertrand-Krajewski, 2005; EPA, 2014; Kesik, 2015; Staufer et al., 2012; Thapa et al., 2019; Mohtlok et al., 2008; Zhang, 2005; 2007). When infiltration and inflow flow together in sewer pipes, they are collectively referred to as I&I. Common sources of I&I are shown in the figure below (King County, 2020).

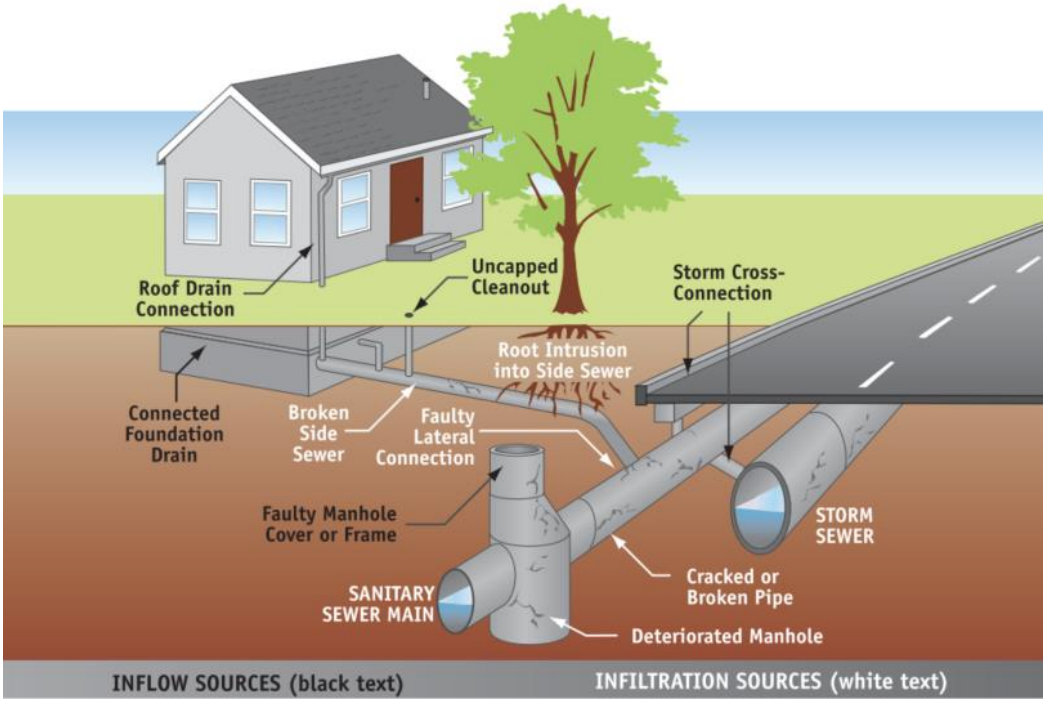

Figure 1.5 Sources of infiltration and inflow are depicted in this diagram published by King County, Washington (King County, 2020).

Notably, a study of 54 sewersheds found I&I rate and pipe age to be highly correlated (Thapa et al., 2019). I&I susceptibility also depends on sewer type, soil type, local climatic conditions, existing municipal infrastructure, and the intensity, frequency, and duration of extreme rainfall events (Kesik, 2015; Thapa et al., 2019). For instance, peaks in inflow are directly related to rainfall, while infiltration changes slowly based on hydrological context (Wittenberg and Aksoy, 2010). If the water table never rises enough to interact with sewer pipes (usually 4-6 feet), groundwater infiltration will never occur.

Infiltration and Inflow can significantly impact total watershed outflows and the entire urban watershed budget. The study by Bhaskar & Welty (2012), which investigated the water budget for urban watersheds in Baltimore, Maryland, found that urbanization decreased ET. However, the resulting excess water leaked into sanitary sewer pipes and eventually WWTPs rather than recharging groundwater. The I&I acted as an additional watershed outflow in some cases, but as inflows in others. In a watershed receiving an average of 1,118 mm per year of precipitation, they estimated annual losses of 300-465 mm per year from I&I. The authors additionally found that total I&I may vary greatly over small distances. For example, pipe age and cracks might vary between two streets depending on maintenance history.

Although excessive I&I only causes a quarter of reported SSO events in the United States, those events comprise almost three quarters of the overall SSO volume discharged (EPA, 2004). These incidences endanger both human and environmental health by releasing contaminants into streams (EPA, 2004; 2014; Kesik, 2015; Zhang, 2005). A Report to Congress on the Impacts and Control of CSOs and SSOs (EPA, 2004) describes the contaminants in detail. Threats to human health found in sewage include more than 120 intestinal viruses (ex:

poliovirus, infectious hepatitis virus, and coxsackie virus), parasites (ex: helminths, giardia and cryptosporidium), and bacteria (ex: E. coli and salmonella). The environment is threatened by raw sewage in the following ways: organic matter depletes dissolved oxygen; total suspended solids degrade ecosystem health and increase turbidity; toxic chemicals reduce biological diversity, productivity, and biomass; excess nutrients cause eutrophic conditions; floatables (trash and debris) cause entanglement or ingestion. These pollutants negatively impact five protected uses of waterways, as defined by the Clean Water Act: aquatic life support, drinking water supply, fish consumption, shellfish harvesting, and recreation.

The effects of I&I are expensive if they evoke legal action, destroy real property, and/or impact municipal wastewater systems. Municipalities face increased operational costs when I&I increases the volume of water being processed at wastewater treatment centers (Wittenberg and Aksoy, 2010). The increased flows cause lower efficiency, elevated energy consumption, higher organic loads, and equipment maintenance (Wittenberg and Aksoy, 2010). Eventually, capacity expansion projects may be necessary (Lanning and Peterson, 2012; EPA, 2014; Rodel, 2017; Zhang, 2005). Ultimately, the American Water Works Association estimates the cost of maintaining and expanding water systems will cost at least one trillion US dollars over the next 23 years (AWWA, 2018).

Professionals working to prevent SSOs and minimize WWTP operation and maintenance costs often seek to quantify I&I at specific points within the sewer system using in-pipe flow meters. Localized I&I estimates allow managers to isolate parts of the sewer system in need of rehabilitation or replacement and later enable quality control by comparing I&I before and after rehabilitation projects. Pipe flow data is also used to forecast peak flows during storm events, which in turn inform associated emergency response and financial planning. Also, municipalities

can more accurately report the value of their wastewater collection systems to the U.S. EPA when using pipe flow data (Zhang, 2005). Managers need a simple, inexpensive, fast method of quantifying I&I at various spatial and temporal scales (Lanning and Peterson, 2012; EPA, 2014; Rodel, 2017; Mohrlok et al., 2008; Zhang, 2005).

Calculating urban water budgets (Equation 5) without adequate I&I measurements forces gross assumptions and jeopardizes the integrity of the budget itself. I&I contributes a significant amount of water to the urban water budget, and I&I must be quantified before water distributed out of the basin via IBTs can be appropriately calculated.

1.4.2 *Quantifying I&I*

Generally, water managers seek to measure the "I/I ratio" (the ratio of rainfall that becomes I&I) (Zhang, 2005). The EPA advises wastewater systems managers on how to calculate an I/I ratio in their "Guide for Estimating Infiltration and Inflow." First, they describe data collection. At least a year of measurements is recommended. Flow data, which can be obtained from municipalities' in-sewer flow monitors, is used to calculate the Average Dry Weather (ADW) flow and the Average Wet Weather Flow (AWW). ADW is defined as "flow during a period of extended dry weather… seasonally high groundwater," including sanitary flow and infiltration but excluding industrial and commercial flows. AWW is the average flow for one week of significant rain. Second, infiltration is estimated by averaging the nighttime flows during dry weather conditions with peak groundwater infiltration. Third, base sanitary flow is calculated using two methods: (1) subtract estimated infiltration from the average daily dry weather wastewater flow, and (2) review of water usage records during times of minimal outdoor water uses. Fourth, the rate and volume of inflow are estimated by differencing the base sanitary flow infiltration data from wet weather flow data.

While engineers have long been estimating I&I according or similarly to the EPA guidelines, many researchers argue that those methodologies are statistically questionable (Zhang, 2005; 2007). Zhang (2005, 2007) argues the shortfalls are based on three main shortcomings. First, dry weather flow (when flow data is not affected by rain events) is used as the reference baseline but is highly variable. Flow can be variable even without any rain events, so using dry weather flow as a baseline can lead to unstable results. Second, data is collected and compared in arbitrary that destroy "the stochastic structure in the observed data." For example, the I&I estimates can be highly variable and are based on rain events of different durations and intensities. Additionally, if rain duration and wetness are not considered when analyzing flow data, I&I can be overestimated. Third, complexities in the data caused by flow monitoring instrument limitations cannot be appropriately dealt with. Flow meter readings taken when a certain velocity threshold within the pipe is exceeded may cause error, for instance. In all, estimates are unstable, and tests taken under similar circumstances yield profoundly different results, yielding them unreliable.

One study adjusted the EPA methodology to find the I&I per length of sewers in one sewershed. To do so, they first calculated potential extraneous flow (maximum I&I that could leak into the SSS) by multiplying precipitation by the difference between total and paved areas. Then, they calculated actual I&I by dividing the difference between actual sewage flow and water consumption rates by the length of the sewer system (Lanning and Peterson, 2012). This methodology makes several flawed assumptions: (1) All drinking water metered at homes go into the sanitary sewer; (2) Precipitation values from a meter in one location is representative of large areas; and (3) Permeability of impervious surfaces is zero (Lanning and Peterson, 2012). This methodology is useful for municipalities themselves but not wholly reasonable for outside

researchers in municipalities that refuse to share sewer maps due to security issues. Zhang (2005, 2007) proposes using a basic regression approach with autoregressive errors for calculating I&I which attempts to avoid flawed assumptions and stochastic unreliability.

1.5 Study Objectives

I&I is inherently difficult to predict because it depends on so many variables, including but not limited to the type of weather event, climate, groundwater characteristics, ground cover, population dynamics, age and capacity of infrastructure, and soil types. Previous reports suggest that magnitudes of I&I within urban watersheds may be strongly correlated with attributes of the sewer-pipe system, or with attributes of the urban landscape. However, the applicability of these relationships across physiographic regions and different urban settings is unknown. The goal of this thesis is to determine whether variations in I&I that exist among urban watersheds, and which are often unmonitored and unknown, can be reliably linked to these infrastructure and landscape attributes. In doing so, this research will expand the breadth of watersheds for which these putative relationships have been rigorously examined.

The research has two specific goals:

(1) Quantify I&I in the South River Watershed.

(2) Examine watershed attributes for correlations with I&I.

2 METHODOLOGY

2.1 Study Area

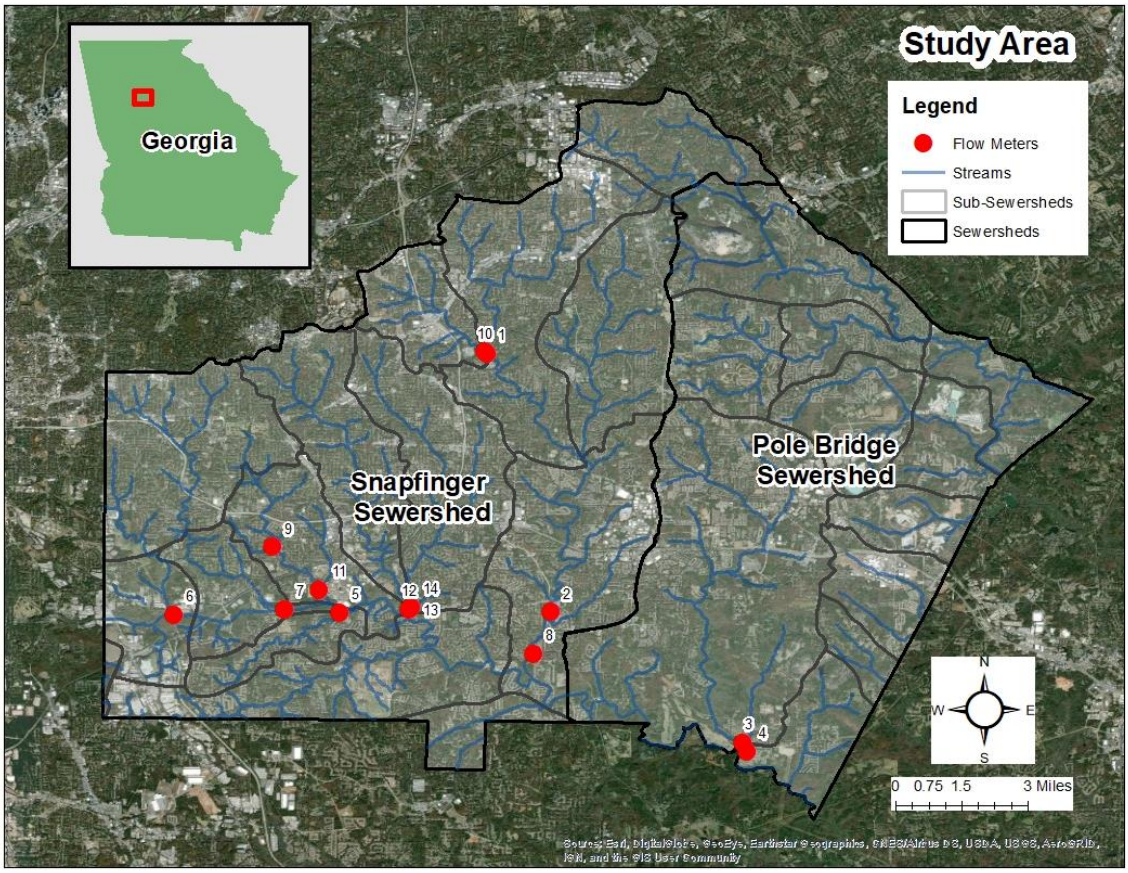

Figure 2.1 The study area within DeKalb County, GA encompasses the Snapfinger and Polebridge sewersheds. The streams found within these sewersheds are part of the South River Watershed. Blue lines indicate streams, red dots indicate flow meters used in this study, grey lines indicate sub-sewershed (smaller units within sewersheds) boundaries, and dark black lines indicate sewershed boundaries.

This study focuses on the intersection between DeKalb County, GA, and the South River Watershed, which lies within the Piedmont physiographic region of Georgia (see fig. 2.1). The Piedmont region is characterized by hilly terrain and Paleozoic-era igneous and metamorphic rocks with unconfined, crystalline-rock aquifers (Gordon and Painter, 2018; Rose and Peters, 2001). Figure 2.2 shows the rock type configuration in DeKalb County. The soils in this hilly

part of the Piedmont region vary between upland and lowland areas. The highland hillslopes have shallow aquifers with less than one meter of soil plus regolith thickness; the Inceptisol and Ultisol soil tends to be well-drained due to their loamy surface and clayey subsoil. Lowland riparian zones have deeper aquifers with loamy and variably well-drained sandy loam soils; the soil plus regolith thickness is generally less than or equal to five meters (Aulenbach and Peters, 2018; Peters and Aulenbach, 2011).

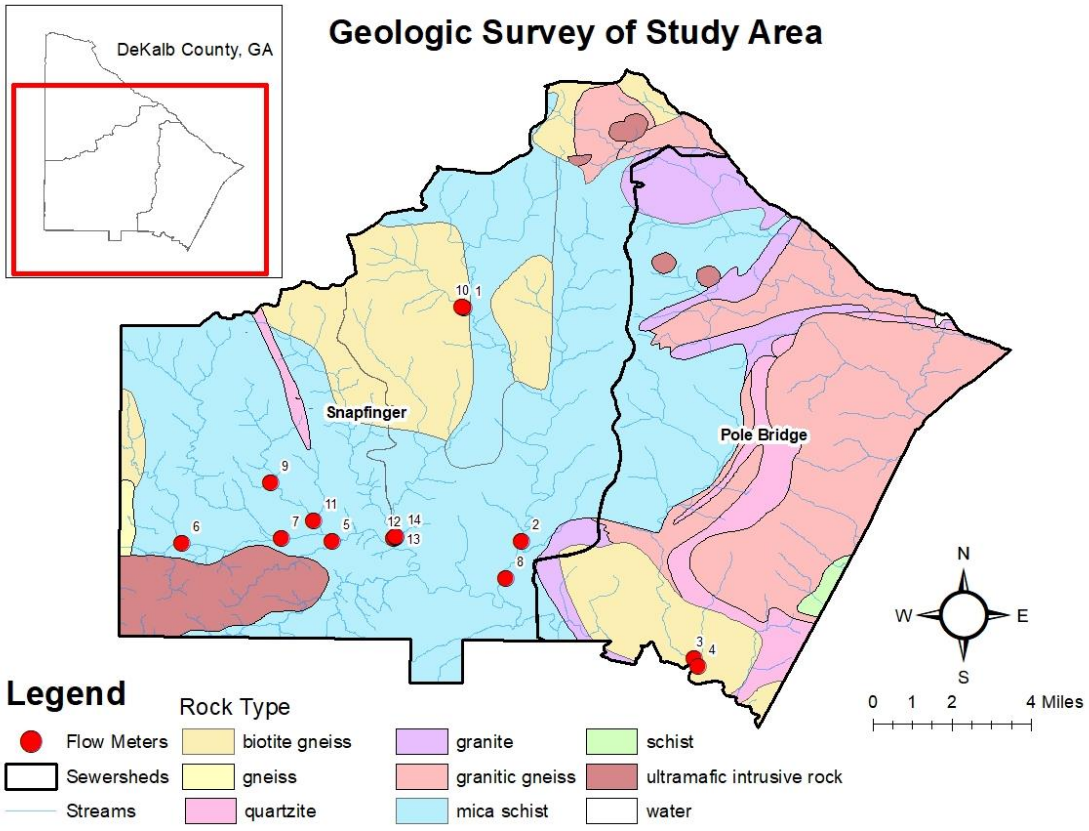

Figure 2.2 This map shoes the primary rock type configuration in the study area.

Absent urbanization/ development, the most common land cover in Metro-Atlanta is forest (Peters, 2009). Land cover within the study area is variable (Fig. 2.3); in 2016 about 59% of land was developed and 33% was forested. Approximately 2% of the overall study area is greater than 90% impervious based on 2016 data (Fig. 2.4).

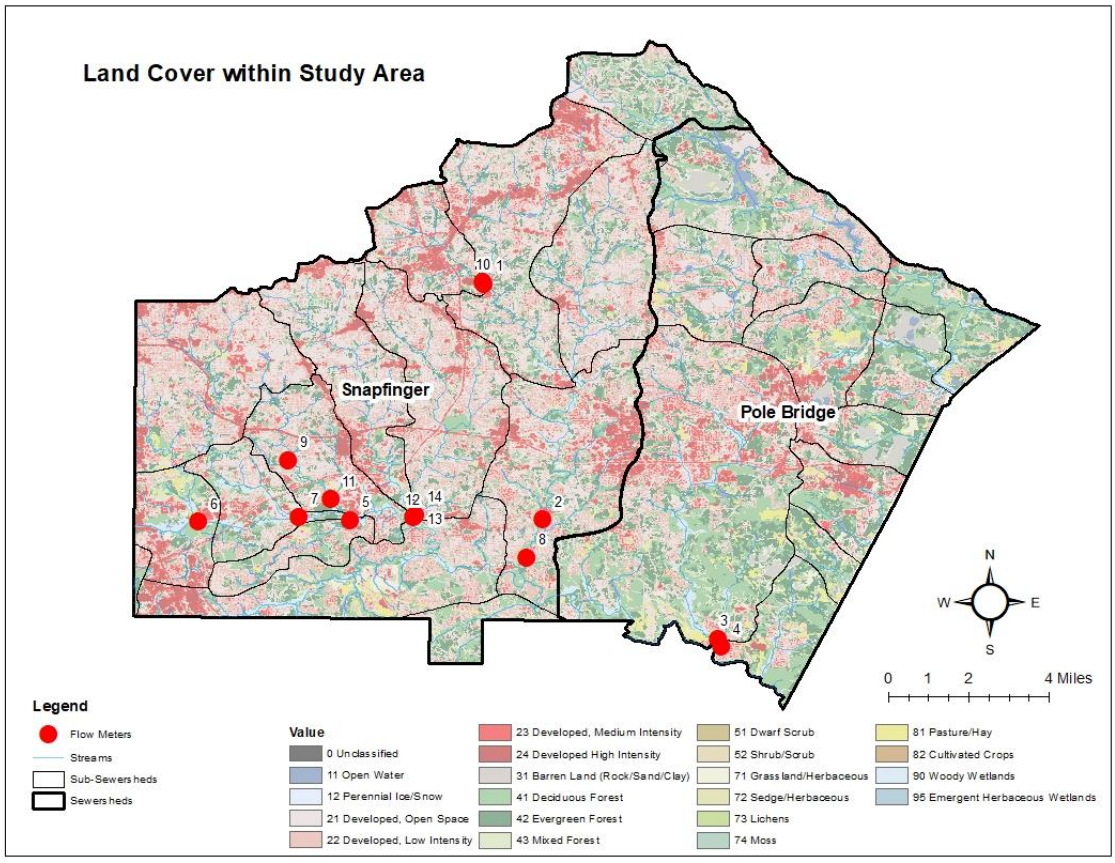

Figure 2.3 Land cover within the Snapfinger and Pole Bridge sewersheds from NLCD2016.

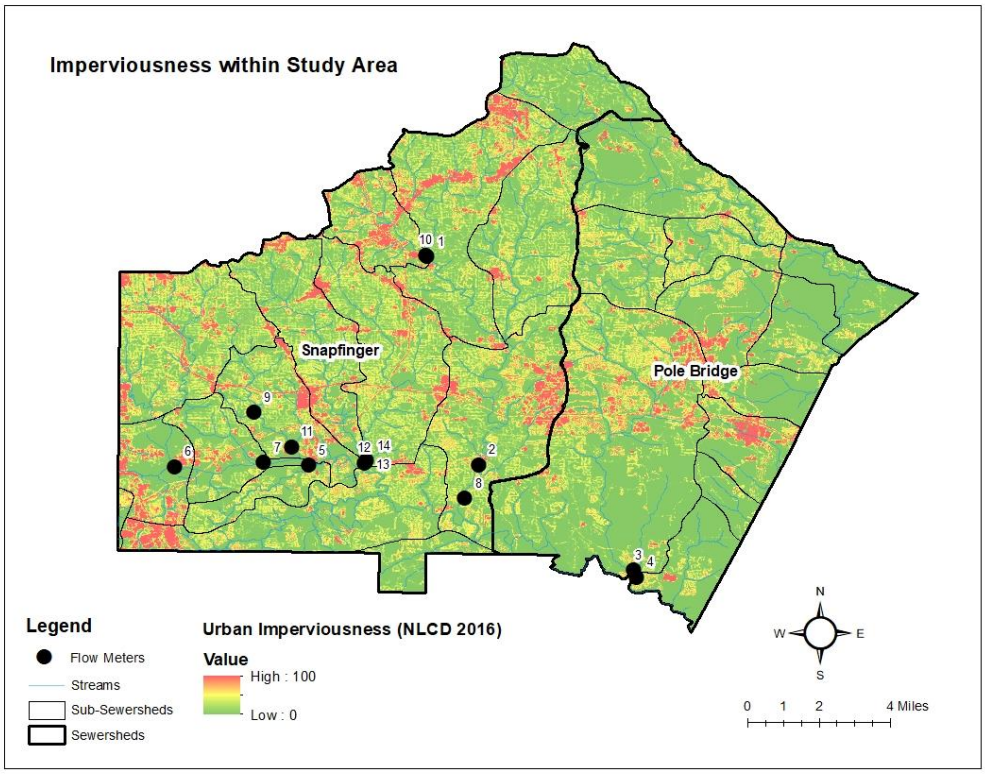

Figure 2.4 Imperviousness within the Snapfinger and Pole Bridge sewersheds from NLCD2016.

The climate in Metro-Atlanta is humid continental to subtropical, so summers are generally hot while winters are cold and wet. Precipitation is evenly distributed throughout the year, averaging about 127 cm/ 50 inches per year (Peters, 2009), although winter precipitation events are typically long and low intensity while summer storms are short and intense (Aulenbach and Peters, 2018). Studies in Panola Mountain Research Watershed, located outside the study area immediately south of the Pole Bridge sewershed boundary, reveal water storage increases between November and March, decreases between April and August, and equal increases/ decreases September through October (Aulenbach and Peters, 2018). Hydrologic droughts and floods are common in the Piedmont region (Seager et al., 2009). Metro-Atlanta

watersheds persistently suffer from urban flooding, partially due to high imperviousness (Ferguson and Ashley, 2017; Diem et al., 2018).

The South River Watershed (SRW) is part of the headwaters of the Upper Ocmulgee River Basin and encompasses 544 square miles of land, including parts of six counties. The South River itself is about 60 miles long and flows into the Ocmulgee River, Altamaha River, and eventually drains into the Atlantic Ocean.

DeKalb County is in Metro-Atlanta, one of the country's fastest-growing urban areas (Diem et al., 2018). It is 267.58 square miles large and encompasses 13 cities, including parts of the City of Atlanta. DeKalb County is home to 753,253 people; 53.9% are Black, 29.1% are White, 8.6% are Hispanic, and 6.4% are Asian (Neighborhood Nexus, 2017). Residents are densely populated at about 2,585.7 people per square mile. The Atlanta Regional Commission (ARC) expects DeKalb county to experience rapid growth; between 2015 to 2040, they forecast a 22% population increase, or a net change of almost 156,000 people over 25 years (ARC, 2015).

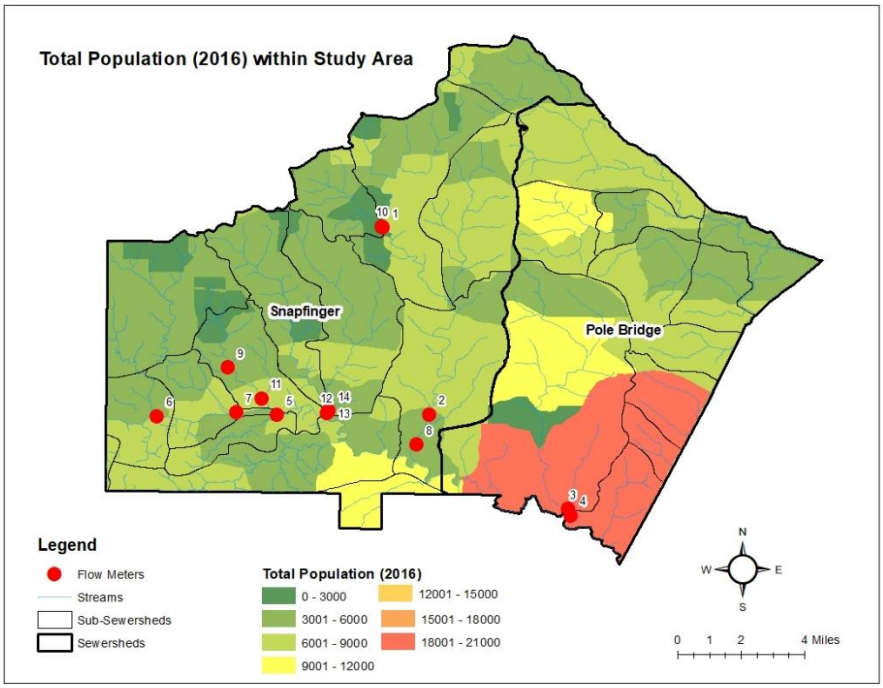

Figure 2.5 Total Population (2016) within the study area.

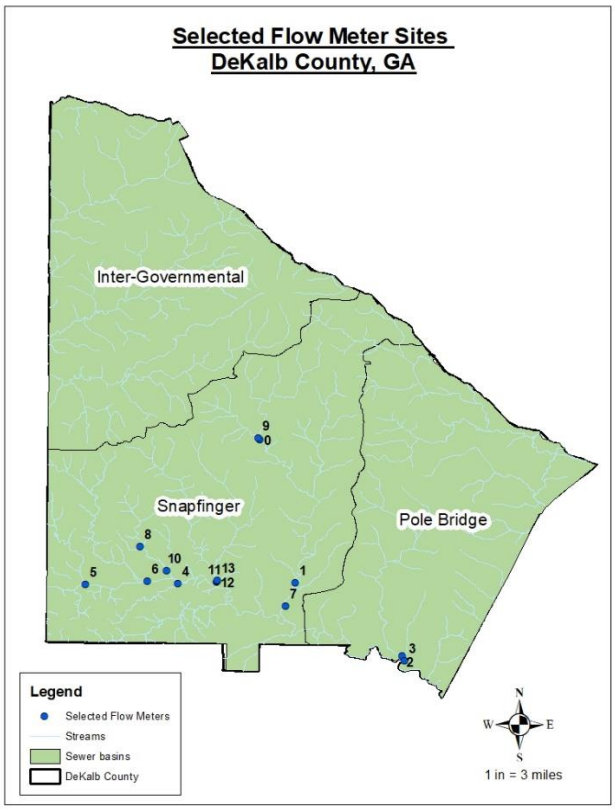

Figure 2.6 DeKalb County has three sewersheds (shown as a sewer basin in this map), but only Snapfinger and Pole Bridge are within the South River Watershed.

DeKalb County is divided into three sewersheds: Intergovernmental, Snapfinger, and Pole Bridge (fid. 2.6). In this study, two sewersheds that overlap with the SRW, Snapfinger and Polebridge, are investigated. In 2015, Snapfinger sewershed contained around 1,098 miles of sanitary sewers and 25,100 manholes; two areas (1/3 Cobb Fowler Creek sewershed and the entire Upper Stone Mountain sewershed) were exclusively served by septic tanks. Pole Bridge sewershed contained around 398 miles of sanitary sewers and 10,600 manholes (DeKalb DWM, 2015a). The age of the County's wastewater control and treatment facilities are reported as the following: 16% is greater than 50 years old, 48% is 25-50 years old, and 36% is less than 25% years old (Consent Decree, 2010). A request for access to a pipe network map of the study area

was denied by DeKalb County. Most of the sewer system consists of gravity pipes that follow streams, so streams were used as a rough estimate of pipe locations (DeKalb DWM, 2015b).

2.2 Data Resources

The analysis utilizes time-series measurements of precipitation and pipe-flow rates obtained through open-records request, and that are collected as part of the DeKalb County Department of Watershed Management's Capacity, Management, Operations, and Maintenance Program (DeKalb DWM, 2015b). That monitoring network includes approximately 200 monitoring locations within DeKalb County. We selected 14 of these locations that lie within the boundaries of the South River watershed, and that were most closely located to either a USGS stream gauging site or a confluence of a tributary with the main stem of the South River. The former criteria enables the most defensible comparisons of I&I magnitudes with the overall magnitude of streamflow discharged from a particular land area, while the latter allows for the most defensible comparisons of whole-sewershed I&I among tributary watersheds with varying size, population density, and landscape attributes.

Flow rates within sanitary-sewer pipes were monitored with Teledyne ISCO LaserFlow sensors, which utilize both laser and acoustic technologies for monitoring depth [L], velocity [$L\ T^{-1}$], and flow [$L^3\ T^{-1}$]. The manufacturer's datasheet reports a typical accuracy of +/- 4% of the flow measurement. The sensors were logged at 15-minute intervals, providing a near-instantaneous estimate of free-surface flow within the pipe (hereafter referred to as pipe flow) that was reported in gallons per minute. Initial review of the time series of data showed infrequent occurrences of zero, or negative, flow values, which were apparently due to episodic sensor malfunction. These negative and zero values were removed from the data prior to further analysis. As such, the total length of time series from all 14 monitoring locations varies; their

length also varies due to different total length of records, which ranges from approximately 12 – 20 months (see Table 1). We addressed this where appropriate by comparing normalized metrics of I&I (e.g., as a percentage of total pipe flow), rather than cumulative sums. Tipping bucket rain gauges were collocated (aboveground) with the in-pipe flow meters. Tip counts and cumulative precipitation estimates from these devices were logged also at a 15-minute interval, and reported in units of inches.

Table 1 Each flow meter site is described by sewershed, sub-sewershed, full site name, and other characteristics.

Sewershed	Sub-sewershed	Area (Sq. Km)	Pop. Density (persons/ sq.km)	Housing Density (units/sq. km)	Land Cover		Flow Monitor Full Site Name
					Total Developed	Total Forested	
Snapfinger	Indian Creek	12.669	1641.12	625.804	80.501	18.643	USF4-15-228-S014-30
							IND1-15-228-S011-24
	Lower Snapfinger	36.88	995.5401	377.2407	70.48	25.912	LSF2-15-065-s014-16
							SFPLNT6-15-034-s089-53
	Blue Creek	7.869	802.7033	324.645	56.657	34.857	BLUE1-15-072-S407-18
	Constitution Area	12.26	307.1445	119.1901	56.27	31.592	CONS1-15-051-S004-18
	Sugar Creek	12.489	703.8935	288.041	56.49	34.882	SUG1-15-074-S022-22.5
	Shoal Creek	24.476	1177.589	555.2393	77.818	20.56	SHO1-15-070-S010-35
	Doolittle Creek	17.9399	1139.151	476.295	71.061	25.103	DOL4-15-107-s045-18
							DOL2-15-088-S017-15
	Cobb Fowler Creek	31.18	824.6052	362.8717	79.276	19.8	CBF1-15-070-S016-30
							CBF2-15-070-S030-15
Pole Bridge	Polebridge Creek	75.145	972.5593	430.866	48.271	41.78	PBPLNT1-11-251-S009-27
	Crooked Creek	12.142	259.2317	97.93722	21.276	59.912	CKC1-11-230-S281-30

2.2.1 *Quantifying infiltration and inflow of precipitation and groundwater into sanitary-sewer pipes*

Our approach to quantifying I&I included three steps. First, we identified intervals within the time series of pipe flow that occurred during precipitation events, or for some specified period of time (hereafter referred to as lag time) after precipitation had ceased. A duplicate time series was created where pipe flow during these time intervals was assigned "NaN". Second, we used a method of statistical interpolation to replace those NaNs within the duplicate time series with estimates of what the pipe flow would have been in the absence of precipitation. This can be done reliably because of the cyclical nature of the time series. Third, we subtracted these interpolated values in the duplicate time series from the actual measurements of pipe flow occurring at the same time within the original time series. These differences represent temporally discrete estimates of I&I, which were summed over time to obtain cumulative totals. Each of these steps is elaborated below.

2.2.2 *Step 1: Delineating time intervals where I&I influences pipe flow*

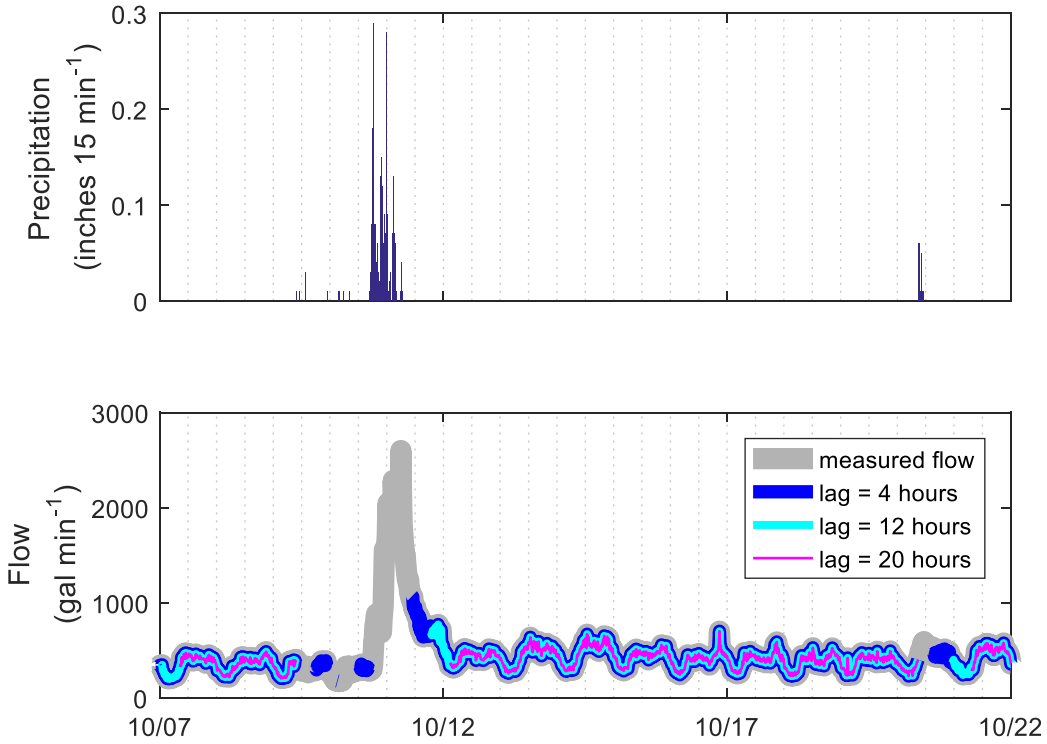

Figure 2.7 Time series of precipitation (top) and pipe flow (bottom) from 10/7/2018 to 10/22/2018. Gray line represents measured flow. Each of three colored lines represent the duplicate data set that results after converting flow values to NaN during, and for variable lag times following, precipitation occurrences. Breaks in the colored lines represent time intervals over which we interpolate the flow that would have occurred in the absence of precipitation, using the moving-window-averaging technique described in the text. I&I is calculated as the difference between measured and interpolated flow during those intervals. For this event, the lag times of 4 and 12 hours will exclude from this calculation a portion of the I&I-induced flow occurring around, and shortly after, 12:00 pm on 10/11/2018, whereas a lag time of 20 hours seems to capture the entire portion of the hydrograph that exhibits some influence of I&I. In contrast, for the small precipitation event on 10/20/2018, the longer lag time of 20 hours here increases the likelihood that some non-zero I&I will be calculated, even though the hydrograph shows little visual evidence of an influence of I&I at all during this event.

Figure 2.7 illustrates one time series of pipe flow, showing multiple days with and without precipitation. On days with no precipitation, the pipe flow follows a well-documented, cyclical pattern that includes minimal values during the night-time and early-morning hours, rapid rise to a relatively high value during mid-morning, a small decline in pipe flow throughout

late morning and the early afternoon, followed by a rise to a second peak in flow during late afternoon and early evening. This pattern is explained by the diurnal variation in wastewater generation by residents of a sewershed. During and after some, though not all, precipitation events, there are marked increases in pipe flow that deviate beyond the typical range of values observed in the absence of precipitation. These deviations more closely resemble the hydrograph of an open channel that is transmitting a precipitation-induced flood wave, rather than the cyclical pattern of flow that results from residential wastewater generation. These deviations are reasonably assumed to reflect the inflow of current precipitation and infiltration of existing groundwater from unconfined aquifers into the sanitary-sewer pipes. The exact proportions of infiltration versus inflow are unknown for any particular event.

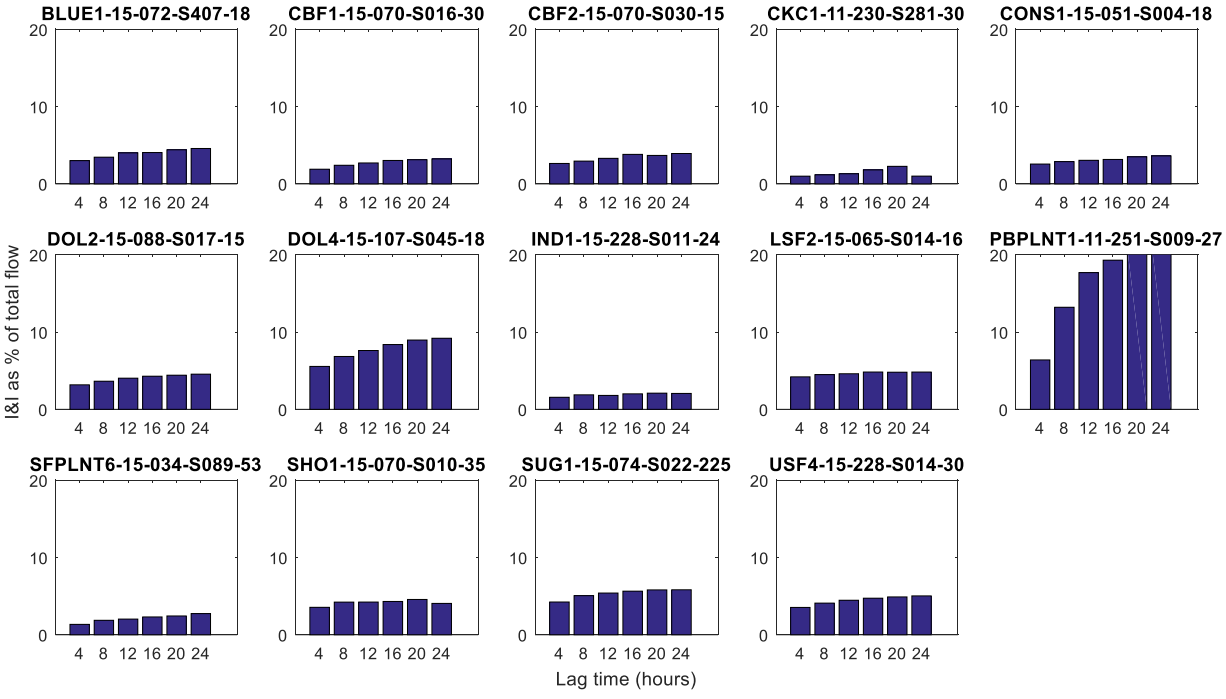

Figure 2.8 Bar graphs showing the dependency of I&I, expressed as a percentage of total pipe flow, on the specified lag time. Titles are identifiers for unique monitoring stations and sensors.

We created a duplicate times series of pipe flow that is identical to the original data, except that we convert numeric values to NaN when (1) precipitation accumulation over the previous 15 minutes was greater than zero, and (2) for a 16-hour lag time following the cessation of precipitation. The lag time was chosen based a simple sensitivity test, whereby we calculated cumulative estimates of I&I, and I&I as a percentage of total pipe flow, using lag times of 4, 8, 12, 16, 20, and 24 hours (fig. 2.8). The dependence of percent I&I on the specified lag time is illustrated in Figure 2.9. With lag times of 4, 8, and 12 hours, it was commonly observed that the range of times during which pipe-flow values were converted to NaN did not fully encompass the observed deviations in flow that resulted from precipitation-induced I&I (see Figure 2.8). This excluded the measured flow values from some time increments being used to calculate I&I, even though their magnitude and deviation from the typical range indicate that they were influenced by I&I (fig. 2.7). With lag times of 16 hours and greater, this type of exclusion was rare.

The sensitivity of percent I&I was also diminished at lag times spanning 16 – 24 hours, although commonly the estimates did continue to slightly increase with lag time. That marginal, positive sensitivity to increasing lag time is attributed to excessive inclusion of time intervals in the calculation of I&I—the opposite problem as described above. Figure 2.7 shows that, when lag time equals 20 hours, the time interval over which pipe-flow values are converted to NaN extends beyond that increment of flow values that deviate markedly from the typical range. Despite the fact that an obvious influence of I&I is unapparent, the measured and interpolated flow values during these time increments will be used to estimate I&I, which is undesirable. Also, for precipitation events that lead to no apparent I&I (e.g. 10/20/2018 from Figure 2.8), a greater lag time increases the probability that a non-zero magnitude of I&I will be calculated,

even though the hydrograph shows little evidence of an effect of I&I at all. Based on this simple sensitivity test, and visual examination of time series, we selected 16 hours as the lag time for all sensors. While no lag time perfectly captures the effect of I&I during each storm event for each sensor, the chosen lag time appears to be appropriate for avoiding systematic underestimation of I&I. We implemented a second calculation, described under section 2.2.3. below, that helps to minimize the effect calculating I&I during periods when the hydrograph shows little evidence of its occurrence.

2.2.3 *Step 2: Interpolating putative flow that would have occurred absent the effect of I&I*

In the second step we interpolated plausible values of pipe flow during those time increments when the actual measured values were replaced with NaN. These interpolated values are meant to represent the likely flow that would have occurred in the absence of precipitation and ensuing I&I. For this purpose we used a simple moving-window-average calculation as shown below:

$$Q_{int,t} = \frac{1}{n}\sum_{i=1}^{i=n} Q[t + \Delta t(i)] \quad (1)$$

where $Q_{int,t}$ is the interpolated flow at time *t*; Δt is a row or column vector of time increments (hours) with length n, and i indexes the individual values within Δt. The initial values assigned to that vector are -48, -24, 24, and 48—the result represents the average pipe flow measured at the same moment in time on the previous, and following, two days. In some cases the measured pipe flow at those preceding and following times may have also been converted to NaN due to the occurrence of precipitation. In that case, the values within Δt were allowed to decrease or increase by increments of -24 and 24, respectively, up to minimum and maximum values of -240 and 240, respectively. In other words, the moving average may be

calculated with preceding and following flow values that occurred up to 10 days before or after the current time, while maintaining $n = 4$. In a very small fraction of cases n was less than four, due to extended periods of very frequent precipitation.

2.2.4 *Step 3: Calculating temporally discrete and cumulative estimates of I&I*

The rate $I\&I_r$ (gal min^{-1}) was calculated at each moment in time delineated in step 1 above as

$$I\&I_r = Q_t - Q_{int,t} \quad (2)$$

where Q_t is the measured pipe flow at time *t*. Given the 15-minute interval of data recording, we assumed this rate was representative of the whole 15-minute period preceding the measurement, and multiply by 15 minutes to obtain the volume $I\&I_v$ (gal) over that time increment. These volumes were summed over time to obtain cumulative $I\&I_{v,tot}$.

Another important observation is that not all precipitation events caused deviations in measured pipe flow that exceed the typical range of values, or exhibit any other evidence of an impact from I&I. The water from a small event during summer, with only a few millimeters of cumulative precipitation, may all evaporate on the same day that it fell as precipitation. The procedure described in the first step above does not specifically exclude these time periods from the eventual estimation of $I\&I_r$. Instead, we utilize a simple filtering approach to discount values of $I\&I_r$ from equation two that are less than the approximate error associated with the statistical interpolation scheme (equation one, section 2.2.3.). Using the duplicate time series generated as stated in section 2.2.3. above, we randomly select 1000 measured values of Q_t. These were all selected from periods of time that had no current precipitation, and that did not fall within the specified lag time; that is, they represent the typical diurnal pattern of pipe flow in the absence of precipitation. Equation one was applied to estimate values of $Q_{int,t}$ at the same 1000 times *t*.

Scatter plots of Q_t versus $Q_{int,t}$ were developed for each sensor, and compared to a line with slope of one. In all cases the residuals appeared randomly distributed about that line, implying no systematic error. We calculated the standard deviation of the residuals, σ, and applied the following condition:

$$if \quad I\&I_r < 2\,\sigma \qquad then \quad I\&I_r = 0 \tag{3}$$

a condition that is based on the approximately normal distribution of the observed residuals around zero, and the assumption that approximately 95% of those residuals should fall within the range -2 σ to 2 σ around the mean.

2.3 Watershed Attributes Analysis

2.3.1 *Pipe age and material*

The attribute table associated with the flow monitor shapefile acquired from DeKalb County DWM lists the material and year in which the pipe attached to the flow meter was installed. There was little variation in materials (12 out of 14 pipes are concrete), but age ranged 57 years. To find correlations between I&I and pipe age, we created a table that included flow monitor name, pipe year of installation, cumulative I&I, percent I&I of total pipe flow, and average rate of I&I.

2.3.2 *Imperviousness*

We downloaded the imperviousness data from the online Multi-Resolution Land Characteristics (MRLC) National Land Cover Database (NLCD2016) as a .tiff file and opened the file in ArcMap 10.6. Then we raster clipped the .tiff file to a polygon of the overall study area (Pole Bridge and Snapfinger sewersheds) as well as individual sub-sewersheds. We saved each area as a new file and followed the same methodology for all files. First, we exported the

imperviousness attribute table as a text file, opened it in Excel, and created a table following the layout shown in Table 2 below.

Table 2 This table is an example of the tables used in imperviousness analysis. The second row provides explanations for each column.

Value	Count	% Impervious	Sum of Count	Total Area Count	% of Total Area
percent impervious, ranging from 0-100% (from attribute table)	The number of raster pixels corresponding to a particular value (from attribute table).	Ranges of values (imperviousness), including ≥95%, ≥90%, ≥85%, ≥80%, …, ≥5%	Sum of counts associated with the values specified in the % impervious column. Calculated using SUMIFS function in Excel.	Sum of all counts in the area.	Percent of the study area that is ≥XX% impervious. $= \left(\frac{sum\ of\ count}{total\ area\ count}\right) * 100$

2.3.3 *Land cover*

The land cover data was also downloaded from the online MRLC NCLD2016 and opened in ArcMap 10.6. We clipped the land cover shapefile to each sub-sewershed polygon and total study area polygon and saved them as new files. Next, we exported the attribute table for each new file into Excel and created a table for analysis. Please refer to Table 3, below, for an example and explanation of each field.

Table 3 This table is an example of the columns used in land cover analysis. The second row provides explanations for each column.

Land Cover Classification	Value	Count	Total Area Count	% of Total Area
The land cover classification corresponding to the values listed in the attribute table. These are found in a legend provided when the data set was downloaded.	The number representing the land cover classification. (From attribute table).	The number of units in the area that are classified as a certain value/ land cover (from attribute table).	Sum of all the counts in the area	The percent of the area that is a certain land cover classification $= \left(\frac{count}{total\ area\ count}\right) * 100$

2.3.4 *Population and housing unit density*

Population and housing density data was obtained from the U.S. Census Bureau's American Community Survey (ACS) 2013-2017 5-year estimates. The densities are calculated by census block group. We uploaded a shapefile for both in ArcMap 10.6 and used the union tool to merge them together. Then we individually clipped the unioned file to each sub-sewershed. The resulting sub-sewershed polygons included both full and partial census block groups, and therefore the overall population/ housing unit densities would be overestimates if simply summed. To account for this, we decided to calculate weighted averages for each sub-sewershed. We exported the population/ housing density attribute tables into Microsoft Excel and created a table for each sub-sewershed. Please see Table 4, below, for an example of how we calculated weighted averages for each sub-sewershed.

Table 4 This table is an example of the columns used in population and housing unit density analysis.

OBJID#	Area of Sub-sewershed (sq. km)	Area of Block Group (sq. km)	Weight	Pop Density (persons/sq km)	Housing Density (housing units/sq.km)	Pop. Density Weighted Average (persons/sq.km)	Housing Density weighted Average (housing units/sq.km)
Object ID assigned to each census block group (from attribute table)	Sub-sewershed area calculated using the geometry calculator in ArcMap	block group area calculated using the geometry calculator in ArcMap	The weight assigned to each block group	Population density of each block group (from attribute table)	housing density of each block group (from attribute table)	**SUMPRODUCT** Sum of the (pop density *weight) for each block group	**SUMPRODUCT** Sum of the (housing density *weight) for each block group
						SUM Sum of all weights	**SUM** Sum of all weights
						WEIGHTED AVERAGE $= \frac{SUMPRODUCT}{SUM}$	**WEIGHTED AVERAGE** $= \frac{SUMPRODUCT}{SUM}$

2.4 I&I Normalization

To account for variations in length of data available for each flow monitor, it was necessary to calculate normalized versions of I&I before intercomparisons could be appropriate. First, we calculated 2019 cumulative I&I by subtracting the I&I value for 12/31/2019 from the value for 1/1/2019. Then we calculated the number of observations where both precipitation and flow were recorded during 2019; we divided 2019 cumulative I&I by the number of observations to find the average rate of I&I (gallons per 15 minutes). We also found the percent I&I of pipe flow by dividing the 2019 cumulative I&I by the 2019 total pipe flow and multiplying by 100.

Table 5 summarizes the raw data, normalization variables, and normalized version of I&I and percent I&I of pipe flow in 2019.

Table 5 shows a summary of the raw data and normalized I&I values for each of the fourteen flow meters. (For more detailed information about each flow meter, return to Table 1 in section 2.2). Malfunctions in flow meters and precipitation gauges sometimes occurred during data collection, which reflected in "days of data" and "number of observations." Days of data refer to the number of days in which data was recorded. Number of observations refers to the number of observations with both flow and precipitation recordings.

Flow Monitor Full Site Name	Range of Data	Days of Data	Cumulative I&I (2019) (gal x 10^7)	Total Pipe Flow (2019) (gal x 10^7)	# of Obs.	% I&I of Pipe Flow (2019)
USF4-15-228-S014-30	7/2/2018 - 1/1/2019, 1/1/2019 - 1/1/2020	270	4.02	92.38	25893	4.36
IND1-15-228-S011-24	7/10/2018 - 1/1/2019, 1/1/2019 - 1/1/2020	357	1.11	55.33	32958	2.01
LSF2-15-065-s014-16	6/21/2018 - 1/1/2019, 1/1/2019 - 1/1/2020	365	0.33	8.54	35039	3.90
SFPLNT6-15-034-s089-53	8/24/2018 - 1/1/2019 1/1/2019 - 1/1/2020	365	7.77	454.40	34945	1.71
BLUE1-15-072-S407-18	6/8/2018 - 1/1/2019, 1/1/2019 - 1/1/2020	365	0.50	11.87	32433	4.24
CONS1-15-051-S004-18	6/20/2018 - 1/1/2019, 1/1/2019 - 1/1/2020	365	0.16	6.70	35040	2.36
SUG1-15-074-S022-22.5	7/5/2018 - 1/1/2019, 1/1/2019 - 1/1/2020	365	0.60	14.76	32433	4.04
SHO1-15-070-S010-35	3/21/2018 - 1/1/2019, 1/1/2019 - 1/1/2020	365	5.25	126.74	35040	4.15
DOL4-15-107-s045-18	3/9/2018 - 1/1/2019, 1/1/2019 - 1/1/2020	365	1.65	24.31	33896	6.80
DOL2-15-088-S017-15	6/18/2018 - 1/1/2019, 1/1/2019 - 1/1/2020	365	0.43	14.56	35040	2.93
CBF1-15-070-S016-30	11/28/2018 - 1/1/2019, 1/1/2019 - 1/1/2020	338	1.89	119.96	32446	1.57
CBF2-15-070-S030-15	3/21/2018 - 1/1/2019, 1/1/2019 - 1/1/2020	365	0.21	6.71	35404	3.18
PBPLNT1-11-251-S009-27	4/4/2018 - 1/1/2019, 1/1/2019 - 1/1/2020	365	0.19	1.37	35040	13.71
CKC1-11-230-S281-30	8/27/2018 - 1/1/2019, 1/1/2019 - 1/1/2020	304	0.08	8.18	27451	1.03

2.5 Statistical Analysis

Each watershed attribute was analyzed for statistical correlation with normalized I&I metrics in the same manner. We created scatter plots relating each attribute with the I&I metrics, plotting a line of best fit using the least squares method. Then, we ran ANOVA linear regression analyses for each relationship to determine if the slopes were significant using p-values and R-squared.

3 RESULTS

Once normalized versions of I&I were calculated for each flow meter, we continued into watershed attribute analysis. Table 6 summarizes the p-values and R^2 values found in the watershed attributes analysis, which is discussed in the remainder of this section.

Table 6 Summary of p-values and R^2 values of relationships between watershed attributes and both (1) percent I&I of total pipe flow and (2) average rate of I&I.

Watershed Attribute	Percent I&I of Total Flow		Average Rate of I&I	
	p-value	R^2	p-value	R^2
Pipe age	0.771	0.008	0.521	0.038
Imperviousness ≥90%	0.260	0.104	0.903	0.001
Imperviousness ≥75%	0.320	0.082	0.593	0.025
Imperviousness ≥50%	0.316	0.084	0.529	0.034
Land Cover- Total Developed	0.643	0.019	0.137	0.175
Land Cover- Total Forested	0.582	0.026	0.154	0.162
Population Density	0.561	0.029	0.117	0.192
Population Density (without PBPLNT meter)	0.124	0.117	0.124	0.201
Housing Density	0.403	0.059	0.123	0.187
Housing Density (without PBPLNT meter)	0.118	0.150	0.118	0.200

3.1 Annual I&I

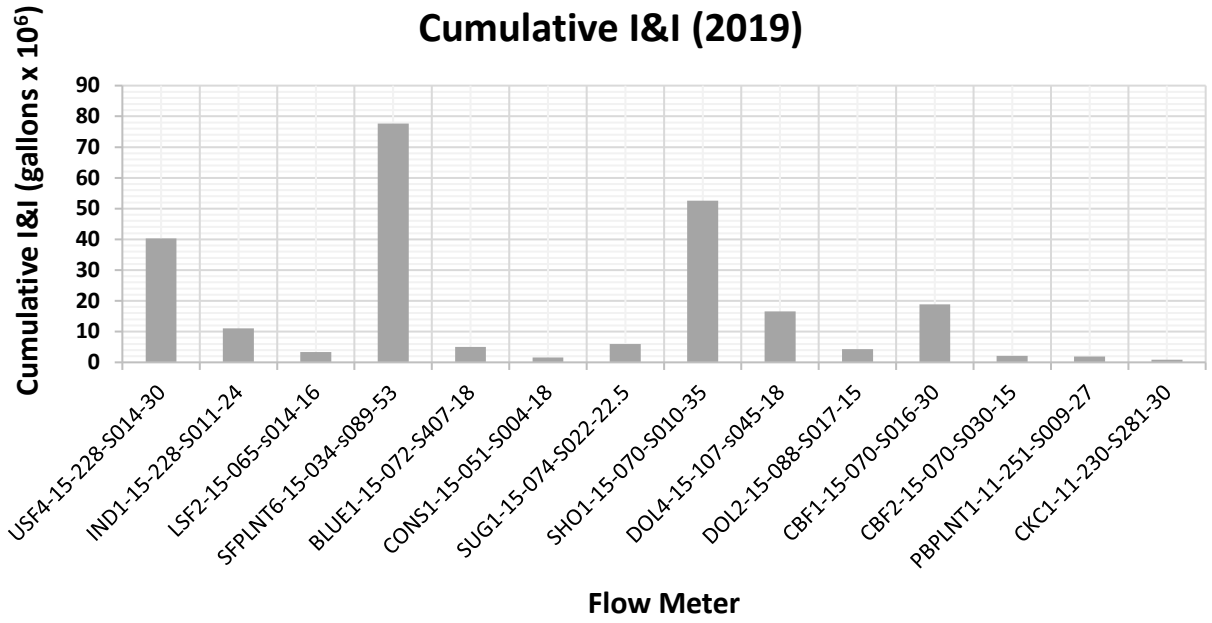

Figure 3.1 Cumulative Annual I&I, normalized by number of observations (where both precipitation and flow were recorded) in 2019.

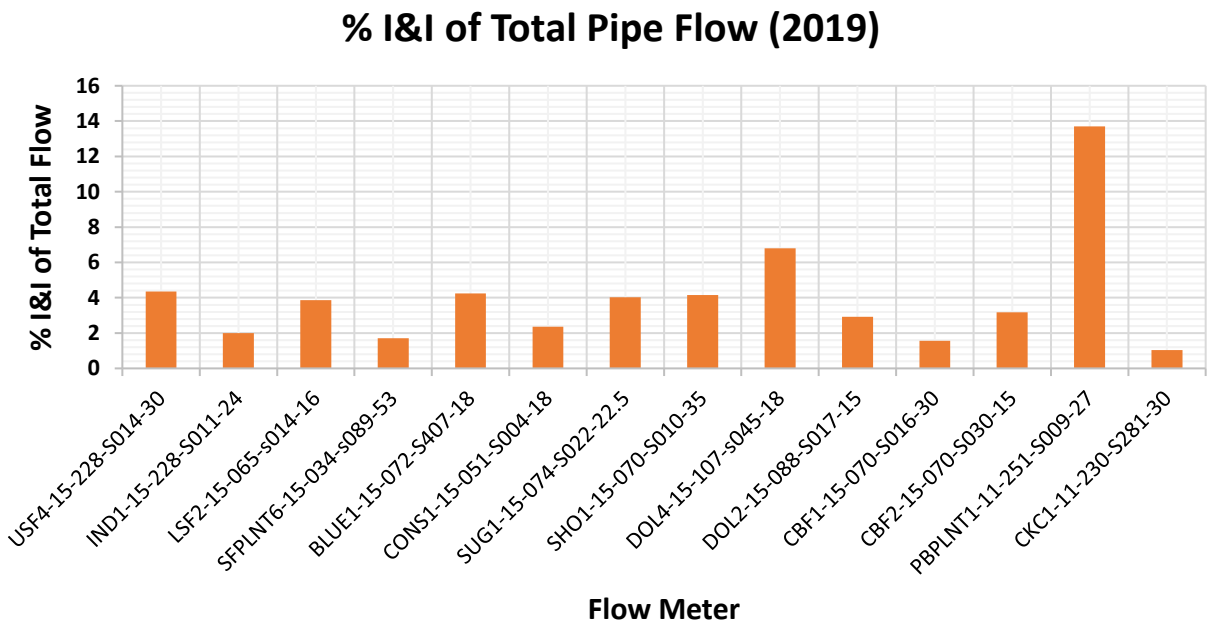

Figure 3.2 Percent I&I of total pipe flow in 2019.

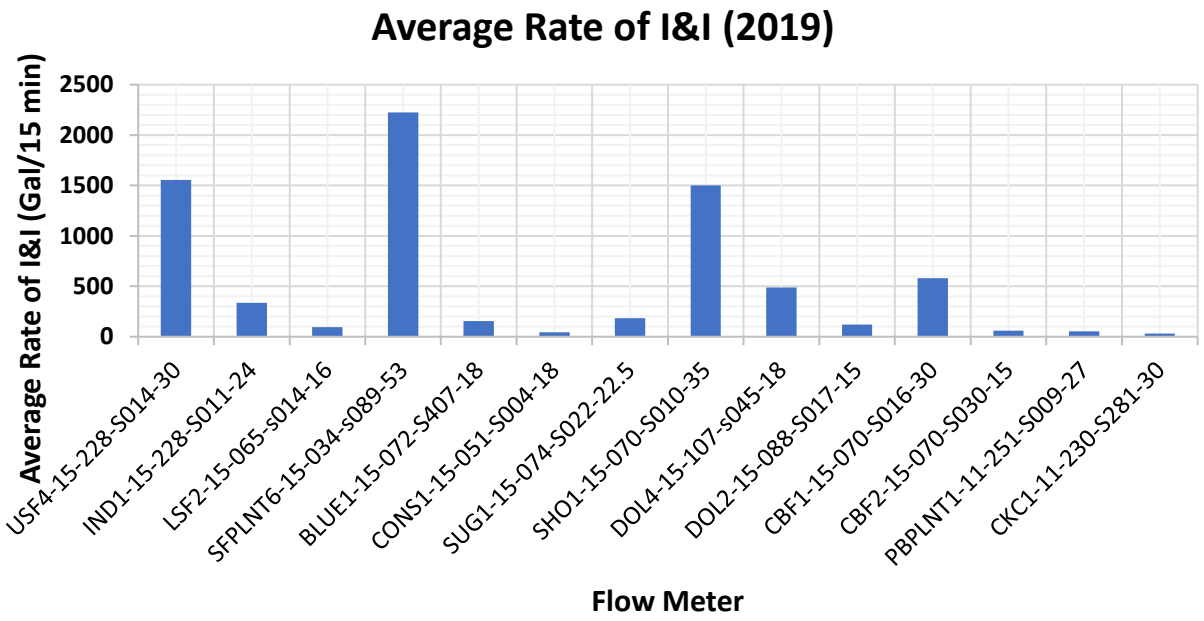

Figure 3.3 Average rate of I&I (gallons per 15 minutes) in 2019.

In general, percent I&I of total pipe flow (fig. 3.2) has a narrow spread, ranging from 1.0% to 6.8%, with one exception being meter PBPLNT1-11-251-S009-27 (14%). The average percent I&I of total pipe flow (fig. 3.3) is 4.0% and the median is 3.52%. The mean average rate of I&I is 530.67 gallons per 15 minutes and the median is 169.41 gallons per 15 minutes. The average annual cumulative I&I (fig. 3.1) is 17.29 x 10^6 gallons and the median is 5.49 x 10^6 gallons.

3.2 Pipe age

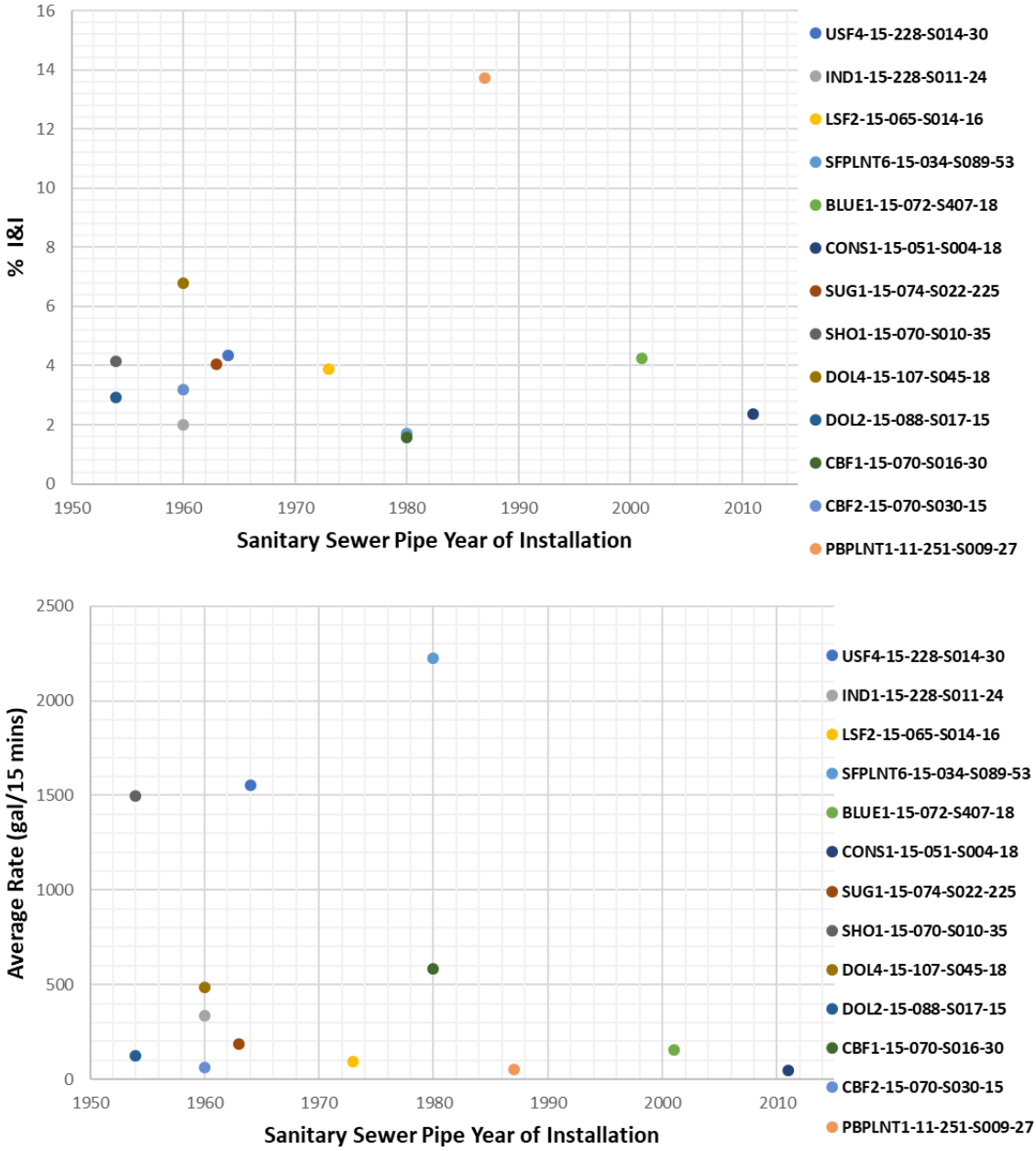

Figure 3.4 Sanitary sewer pipe age versus percent I&I of total pipe flow and average rate of I&I. These scatter plots show the relationship between the age of the pipe in which the flow meter is installed versus percent I&I of total flow and average rate of I&I in 2019. Each data point is specific to a flow meter, shown in the legend. The line of best fit is included and was calculated using the least square method. The R^2 values are approximately 0.01 and 0.18 respectively. Flow meter CKC1-11-230-S281-30 is omitted from these graphs because there was no pipe year available in the data. Please note that the years shown here do not represent the

age of the overall pipe system of each sub-sewershed or metershed; we were not able to acquire that information during data collection.

Twelve of the fourteen flow meters used in this study are installed in concrete pipes, which range between nine and 66 years of age. The average age of installation is 47 years (1972), with a median of 55 years (1964). Figure 3.4 shows the pipe age versus percent I&I of total pipe flow and average rate of I&I. The R^2 values of both data sets, calculated using the least square method, show little correlation between the variables. The p-value for age versus percent I&I, 0.771, and versus average rate of I&I, 0.521, show no significant correlations.

3.3 Imperviousness

Imperviousness is expressed as a percent of sub-sewershed area that is greater than or equal to a degree of imperviousness (either ≥90%, ≥75%, or ≥50%). We calculated imperviousness in degree increments of 5% and used the least square method to test whether any marked differences in correlation exist. Ultimately, we saw little difference in the nineteen R^2 values calculated; the three categories shown here adequately communicate the differences in impervious between sub-sewersheds.

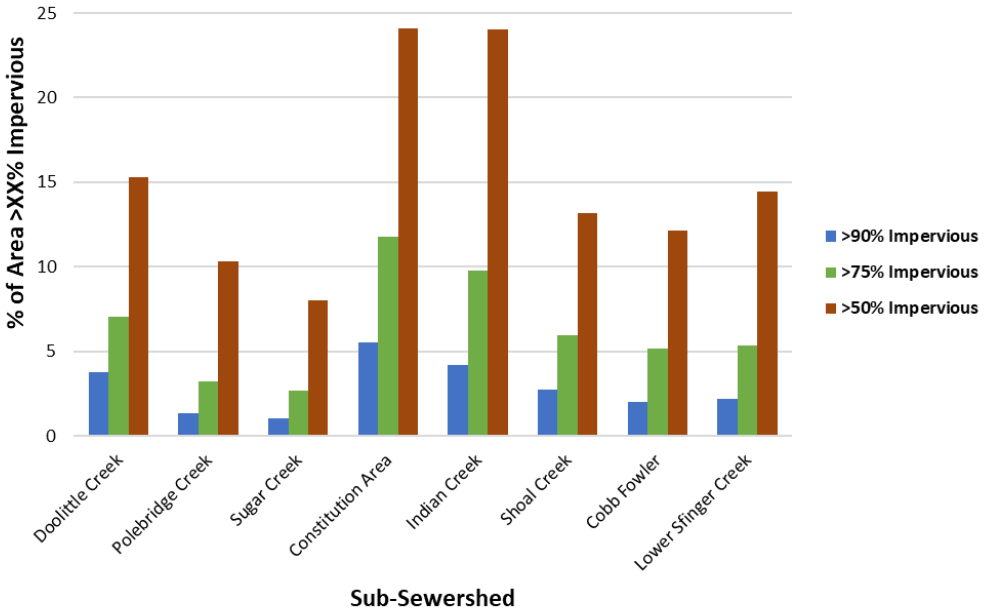

Figure 3.5 Imperviousness by Sub-Sewershed. This bar graph depicts the percent of sub-sewershed area that is greater than or equal to 90%, 75%, and 50% impervious. Note there are only eight sub-sewersheds shown because some of the 14 flow meters are located within the same sub-sewersheds.

The most impervious areas within sub-sewersheds (greater than or equal to 90% impervious) comprise between 0.33-5.50% of total area; between 0.81-12% of sub-sewershed areas are greater than or equal to 75% impervious, and between 5.1-24% of sub-sewershed areas are greater than or equal to 50% impervious. Figure 3.5 depicts the imperviousness of each sub-sewershed. Figure 3.6 plots imperviousness versus percent I&I of total flow. Each flow meter is represented in the scatter plots. Correlation was measured by creating a line of best fit using the least squares method. The R^2 values for each scatter plot are below 0.15 and therefore show little to no correlation between imperviousness and I&I. Also, the p-value for age versus percent I&I, ranging from 0.260-0.360, and versus average rate of I&I, ranging from 0.529-0.903, show no significant correlations.

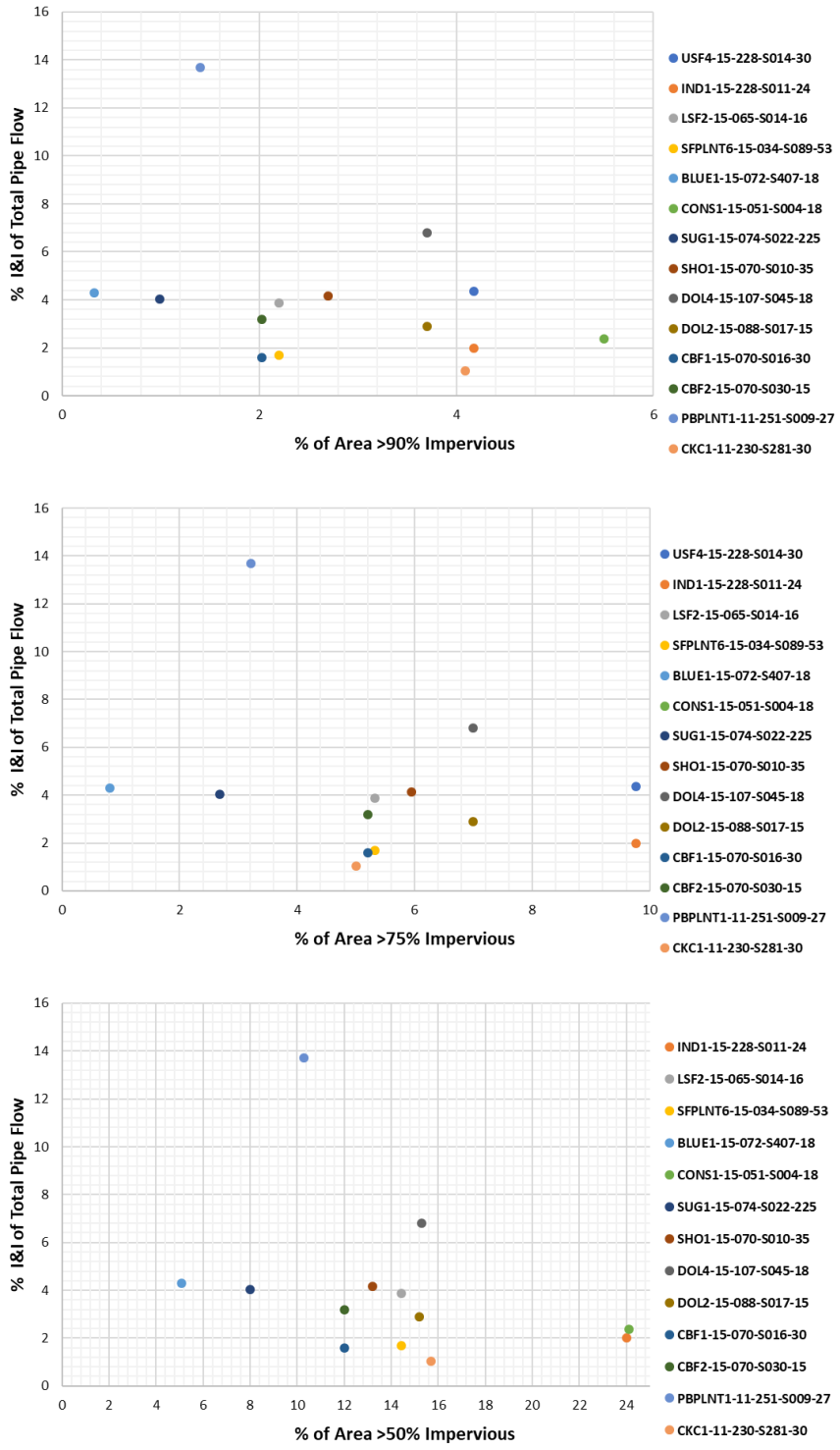

Figure 3.6 These scatter plots show the relationship between percent I&I and percent of sub-sewershed areas that are ≥90%, ≥75%, and ≥50% impervious. Each data point corresponds to a flow meter, and a line of best fit was calculated for each scatter plot using the least square method. The R^2 values are approximately 0.10, 0.08, and 0.08, respectively. When the PBPLNT1 flow meter is omitted, the R^2 values become approximately 0.0042, 0.03, and 0.01.

3.4 Land cover

Table 7 This table lists land cover classifications (from the MRLC NCLD2016) by flow meter. The developed land categories are fractional measures of imperviousness, including developed open space (<20% impervious), developed low intensity (20-49% impervious), developed medium intensity (50-79% impervious), and developed high intensity (80-100%). Please note: some flow meters have identical I&I and land cover classification values because we calculated land cover by sub-sewershed.

Flow Monitor Full Site Name	% I&I of Piped Flow (2019)	% Land Cover (2016)					
		Developed, open land	Developed, Low Intensity	Developed, Medium Intensity	Developed, High Intensity	Total Developed	Total Forested
USF4-15-228-S014-30	4.36	30.2	26.2	16.5	7.6	80.5	18.6
IND1-15-228-S011-24	2.01	30.2	26.2	16.5	7.6	80.5	18.6
LSF2-15-065-s014-16	3.90	28.2	27.8	10.2	4.2	70.5	25.9
SFPLNT6-15-034-s089-53	1.71	28.2	27.8	10.2	4.2	70.5	25.9
BLUE1-15-072-S407-18	4.24	25.7	25.9	4.5	0.6	56.7	34.9
CONS1-15-051-S004-18	2.36	14.5	17.7	14.3	9.8	56.3	31.6
SUG1-15-074-S022-22.5	4.04	30.1	18.4	6.0	2.1	56.5	34.9
SHO1-15-070-S010-35	4.15	38.3	26.3	8.5	4.7	77.8	20.6
DOL4-15-107-s045-18	6.80	30.6	25.0	9.5	6.0	71.1	25.1
DOL2-15-088-S017-15	2.93	30.6	25.0	9.5	6.0	71.1	25.1
CBF1-15-070-S016-30	1.57	35.9	31.2	8.2	4.0	79.3	19.8
CBF2-15-070-S030-15	3.18	35.9	31.2	8.2	4.0	79.3	19.8
PBPLNT1-11-251-S009-27	13.71	19.0	19.0	7.8	2.5	48.3	41.8
CKC1-11-230-S281-30	1.03	9.7	8.3	2.3	1.0	21.3	59.9

Thirteen land cover classifications are represented in the study area and are detailed in Table 6. We divided the classifications into developed land (including open space, and high, medium, and low intensity spaces) and forested land (including deciduous, evergreen, and mixed forest), and used percentages of total area to make comparisons between sub-sewersheds of varying sizes more accurate. In the total study area, 32% was forested while 59% was developed. From greatest to least, the top five classifications in the study area are developed open space, low-intensity developed space, deciduous forest, evergreen forest, and medium-intensity developed space.

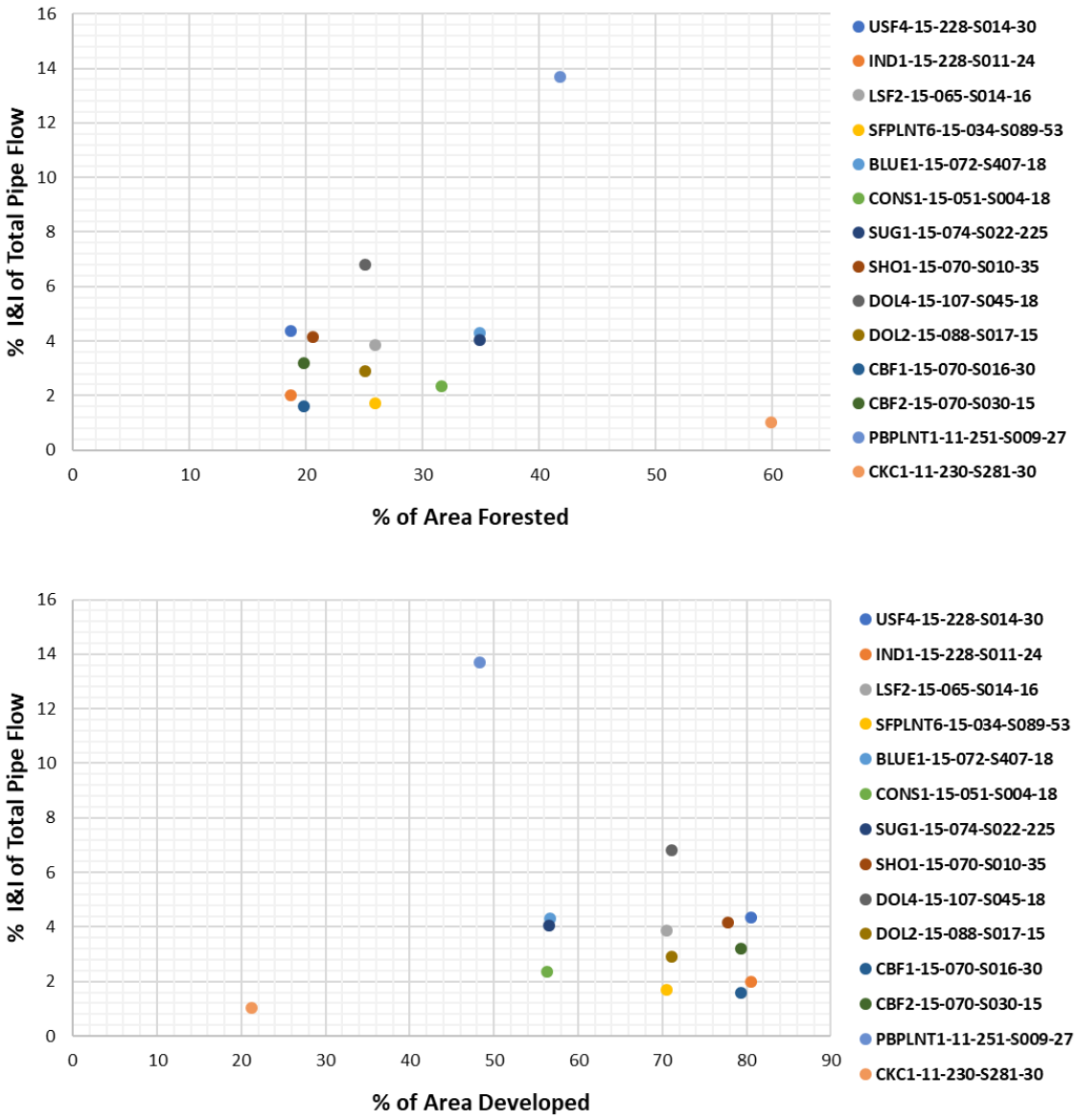

Figure 3.7 These scatter plots show total developed land cover (open land and high, medium, and low intensity) and total forested land cover (deciduous, evergreen, and mixed) vs. percent I&I of total piped flow. Lines of best fit are included and use the least square method. The R^2 values for the lines of best fit are approximately 0.58 (total forested area) and 0.02 (total developed area). Without the PBPLNT1 flow meter, the R^2 values become approximately 0.03 and 0.02, respectively.

Figure 3.7 shows the relationship between land cover (forested or developed) and percent I&I of total pipe flow. Each data point corresponds to a flow meter; correlation was determined using the least squares method. The R^2 values (approximately 0.03 and 0.09) show there is little

to no correlation between land use and I&I. Also, the p-value for total developed land versus percent I&I (0.643) and average rate (0.137) show no significant relationship. Likewise, the p-value for total forested land versus percent I&I (0.582) and average rate (0.154) show no significant correlation.

3.5 Population and housing density

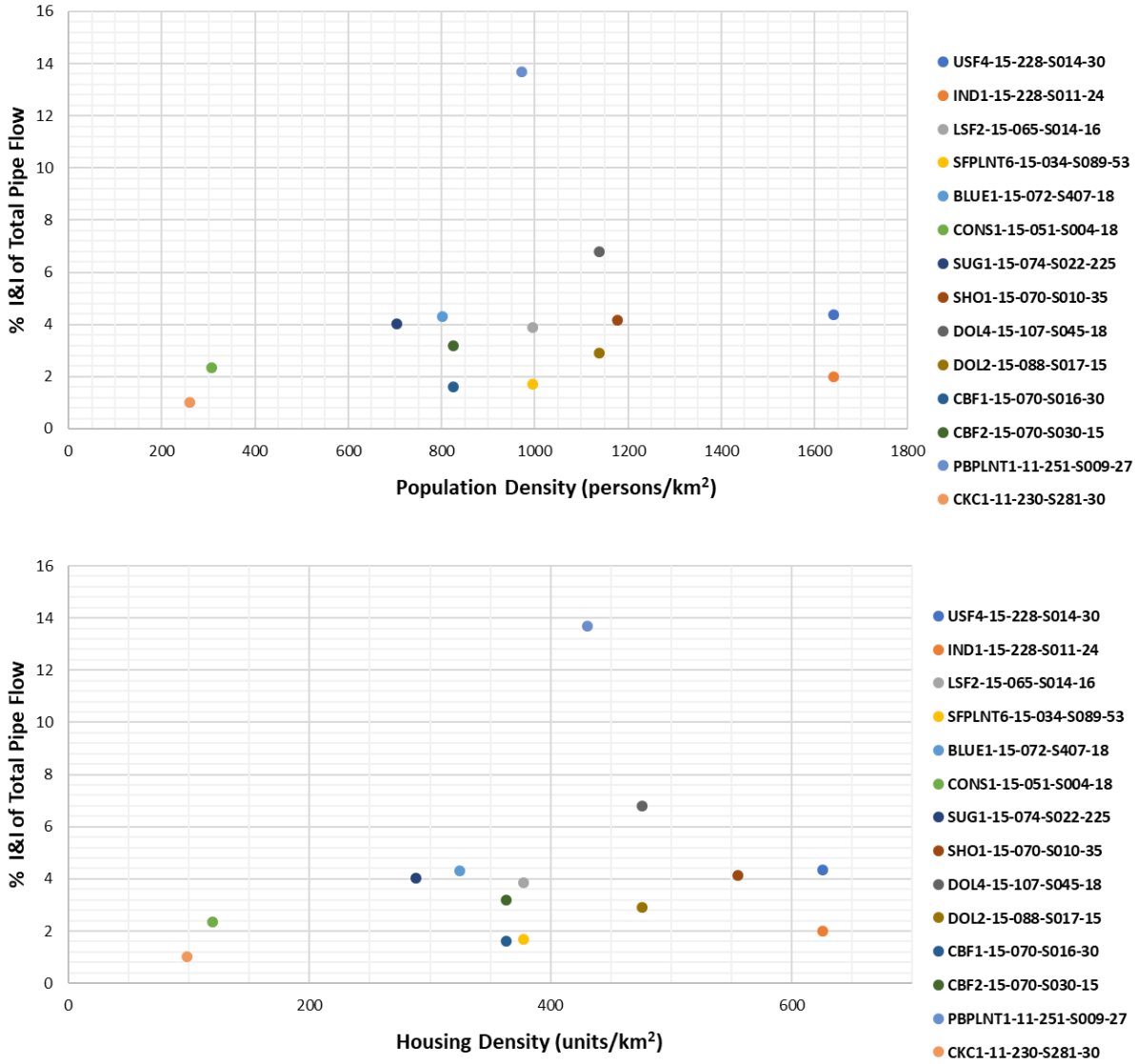

Figure 3.8 These scatter plots show population density (persons per km^2) and housing density (units per km^2) versus percent I&I of total pipe flow. Two lines of best fit are shown per graph: one including the full data set and another that excludes PBPLNT1-11-251-S009-27. The approximate R^2 values of full data sets are 0.03 and 0.06, respectively. When the trend line is calculated without the PBPLNT1 flow meter, the R^2 values become 0.12 and 0.15, respectively.

The final watershed attributes analyzed are population and housing density. We used the U.S. Census Bureau's American Community Survey (ACS) 2013-2015 five-year estimates to find total population and housing units at the block-group level, which were then converted to density values (persons per sq. km and housing units per sq. km). We calculated and used the weighted average of all census blocks within each flow meter's sub-sewershed to prevent over and under estimation that would have resulted from summing the values of each census block (some of the census blocks were barely within sub-sewershed boundaries). Figure 3.8 shows the relationships between population and housing density (weighted averages) and percent I&I of total pipe flow for each flow meter. The scatter plots above include two lines of best fit: one using the full data set, and another excluding the PBPLNT1-11-251-S009-27 flow meter. While the PBPLNT meter may not be an outlier, its I&I value is much higher than all other flow meters studied. When excluding PBPLNT flow meter, the population density approximate R^2 value increases from 0.03 to 0.12 and the p-value decreases from 0.561 to 0.124; the housing density approximate R^2 value increases from 0.06 to 0.15 and p-value decreases from 0.403 to 0.118.

4 DISCUSSION

The range in I&I was relatively small: percent I&I of total pipe flow in 2019 ranged from around 1-14%, but the median was 3.5%. We were somewhat surprised to find little to no correlation between I&I and the watershed attributes investigated (pipe age, imperviousness, land use, housing density, and population density), although the literature offers differing conclusions on whether/ which watershed attributes are accurate predictors or indicators of I&I. The watershed attributes with the most notable correlations appear to be housing and population density (when a meter with high I&I was excluded). Please refer to Table 6 for specific p-values and R^2 values.

In our regression analysis of pipe age and percent I&I of total flow, no significant correlations were found. This finding is interesting, and somewhat surprising, because studies often assume a correlation exists (Chughtai and Zayed, 2010; Thapa et al., 2019) despite the absence of large-scale studies investigating a correlation (Kesik, 2015). Chughtai and Zayed (2007) as well as Thapa et al. (2019) used pipe age to create models predicting wastewater system vulnerability to I&I but did not test to verify a pipe age-I&I rate correlation. For example, Thapa et al. (2019) identified potential I&I prone areas in the city of Youngstown, Ohio by creating mapping models with various weighting schemes of four parameters (pipe age, empirical operating coefficients based on Chughtai and Zayed (2007), soil classifications, and sewer classifications) using spatial data that enabled them to calculate sewer age and classification for individual pipe segments. I&I calculations were not applied to test which model, and therefore which parameter weights, offers the most accurate predictions.

A major limitation affecting our analysis of pipe age and I&I is that we only considered the age of the pipes with flow meters attached- so, about 14 pipes in all. Access to the municipal

pipe network map would facilitate more accurate spatial representation of pipe ages (Thapa et al., 2019), but our request to DeKalb County DWM for the pipe network maps of Snapfinger and Pole Bridge sewersheds was denied. Pipe age within Pole Bridge and Snapfinger sewersheds might be spatially variable for many reasons, including periodic replacement or rehabilitation of malfunctioning pipes and connections. Future studies of pipe age and I&I rate in DeKalb County would benefit greatly from acquiring the pipe network map.

Like pipe age, there is no significant correlation between imperviousness or land use and I&I. Most of the sub-sewersheds we studied were between 55-85% developed and 15-30% forested. Potential errors during data collection and analysis may have impacted our results. The NLCD2016 data is about 83% accurate (Homer et al., 2020), and the error is attributed to weaknesses in differentiating anthropogenic and natural surfaces like concrete and bare soil (Jacobson, 2011; Myeong et al., 2003). Also, conditions in 2019 may not be accurately reflected in the NCLD2016 if significant changes in land cover occurred during the three-year gap.

More watershed attributes could be analyzed using the methodology used in this study. For example, soil type and characteristics (especially those impacting infiltration capacity) may prove an indicator for significant I&I. If the pipe network map is acquired, attributes including average pipe age, pipe length, and pipe material should be further evaluated. Pipe condition, calculated using a multiple regression model developed by Chughtai and Zayed (2007) and used by Jacobson (2011), may yield significant correlation with I&I as well.

Considering the lack of correlation between I&I and the attributes we studied, it is clear that widespread monitoring programs and field testing are imperative in prioritizing sewer rehabilitation and expansion projects. Water resources managers will need to weigh the expense

incurred by constructing and implementing widespread monitoring systems against the long-term benefits, including infrastructure resilience and safeguards of public and environmental health.

5 CONCLUSIONS

Urbanization changes the way water moves through the landscape. Infrastructure-mediated flows impact base flow, groundwater recharge, evapotranspiration, and more. Malfunctions in water collection systems allow water to both infiltrate and inflow into sanitary sewer pipes and overwhelm wastewater treatment systems. If I&I increases pipe flow past carrying capacity, SSOs occur and dump untreated wastewater into streams and landscapes. Public and environmental health both depend on the reduction and mitigation of SSOs.

DeKalb County, Georgia is a community in the Metropolitan Atlanta region with a history of SSOs. The purpose of this study was to calculate I&I in two DeKalb County sewersheds and determine whether several watershed attributes are reliable indicators of I&I hotspots. The main findings are as follows:

- **I&I in the study area comprises approximately 1-14% of total sanitary sewer pipe flow.**
- **The watershed attributes investigated (imperviousness, land use, pipe age, population density, and housing unit density) are spatially variable and, based on regression analysis, have no significant correlation with I&I. They cannot be used as indicators of high I&I or predictors for SSOs.**
- **Since watershed attributes are not reliable indicators of I&I, it is extremely important that water managers have access to widespread sewer system flow monitoring.**

Our findings will be useful for further investigations into the impacts of IMFs on the Atlanta region in part because our methodology for calculating I&I is suitable for solving comprehensive water budgets. Our method also provides an efficient and accurate option for water managers to monitor I&I in their municipalities, which is especially important since basic watershed attributes cannot be used as indicators or predictors.

REFERENCES

Ana, E., Bauwens, W., Pessemier, M., Thoeye, C., Smolders, S., Boonen, I., & De Gueldre, G. (2009). An Investigation Of The Factors Influencing Sewer Structural Deterioration. *Urban Water Journal, 6*(4), 303-312. doi:10.1080/15730620902810902

Anderson, J. R. II. (2010). *The Effects of High Density Septic Systems on Surface Water Quality in Gwinnett County, Georgia.* Georgia State University, Retrieved from https://scholarworks.gsu.edu/geosciences_theses/28

ARC. (2015). *Forecast 2040: DeKalb County*. Retrieved from https://documents.atlantaregional.com/The-Atlanta-Region-s-Plan/pop-employment-forecasts/dekalb-forecast.pdf

ASCE. (2019). *2019 Report Card for Georgia's Infrastructure*. Retrieved from https://www.infrastructurereportcard.org/state-item/georgia/

Aulenbach, B. T., & Peters, N. E. (2018). Quantifying Climate-Related Interactions in Shallow and Deep Storage and Evapotranspiration in a Forested, Seasonally Water-Limited Watershed in the Southeastern United States. *Water Resources Research, 54*(4), 3037-3061. doi:10.1002/2017wr020964

AWWA. (2001). Dawn of the Replacement Era: Reinvesting in Drinking Water Infrastructure. *Association Water Works Association*. Retrieved from https://www.tucsonaz.gov/files/water/docs/Dawn_of_the_Replacement_Era.pdf

AWWA. (2018). Buried No Longer: Confronting the U.S. Water Infrastructure Challenge. *Express Water*, 27-29. Retrieved from https://www.awwaindia.com/portals/pdf%20folder/Express%20Water%20-%20August%202018_Buried_No_Longer.pdf

Baur, R., & Herz, R. (2002). Selective Inspection Planning With Ageing Forecast For Sewer Types. *Water Science And Technology : A Journal Of The International Association On Water Pollution Research, 46*(6-7), 389-396. Retrieved from https://search.ebscohost.com/login.aspx?direct=true&AuthType=ip,shib&db=cmedm&AN=12381016&site=eds-live&scope=site&custid=gsu1

BC Water & Waste Association. How Do Our Water Systems Work? (2020). Retrieved from http://www.valueofwater.ca/water-facts/how-do-our-water-systems-work/

Belhadj, N., Joannis, C., & Raimbault, G. (1995). Modelling Of Rainfall Induced Infiltration Into Separate Sewerage. *Water Science and Technology, 32*(1), 161-168. doi:10.2166/wst.1995.0036

Bhaskar, A. S., & Welty, C. (2012). Water Balances along an Urban-to-Rural Gradient of Metropolitan Baltimore, 2001-2009. *Environmental and Engineering Geoscience, 18*(1), 37-50. doi:10.2113/gseegeosci.18.1.37

Bhaskar, A. S., & Welty, C. (2015). Analysis Of Subsurface Storage And Streamflow Generation In Urban Watersheds. *Water Resources Research, 51*(3), 1493. Retrieved from http://ezproxy.gsu.edu/login?url=http://search.ebscohost.com/login.aspx?direct=true&db=edb&AN=102165986&site=eds-live&scope=site

Bhaskar, A. S., Beesley, L., Burns, M. J., Fletcher, T. D., Hamel, P., Oldham, C. E., & Roy, A. H. (2016a). Will It Rise Or Will It Fall? Managing The Complex Effects Of Urbanization On Base Flow. *Freshwater Science, 35*(1), 293-310. doi:10.1086/685084

Bhaskar, A. S., Hogan, D. M., & Archfield, S. A. (2016b). Urban Base Flow With Low Impact Development. *Hydrological Processes, 30*(18), 3156-3171. doi:10.1002/hyp.10808

Bonneau, J., Fletcher, T. D., Costelloe, J. F., & Burns, M. J. (2017). Stormwater Infiltration And The 'Urban Karst' – A Review. *Journal of Hydrology, 552*, 141-150. doi:https://doi.org/10.1016/j.jhydrol.2017.06.043

Borden, S. (2014). *Thirsty City : Politics, Greed, and the Making of Atlanta's Water Crisis*. Albany: State University of New York Press.

Burns, D., Vitvar, T., McDonnell, J., Hassett, J., Duncan, J., & Kendall, C. (2005). Effects Of Suburban Development On Runoff Generation In The Croton River Basin, New York, USA. *Journal of Hydrology, 311*(1-4), 266-281. doi:10.1016/j.jhydrol.2005.01.022

Cahoon, L. B., & Hanke, M. H. (2017). Rainfall Effects On Inflow And Infiltration In Wastewater Treatment Systems In A Coastal Plain Region. *Water Science and Technology, 75*(8), 1909-1921. doi:10.2166/wst.2017.072

Chughtai, F., Zayed, T. (2007). Sewer Pipeline Operational Condition Prediction Using Multiple Regression. *Pipelines 2007,* 1-11doi:10.1061/40934(252)18

City of Tampa, Florida. (2020). Pipes: Progressive Infrastructure Planning To Ensure Sustainability. Retrieved from https://www.tampagov.net/pipes

Consent Decree- DeKalb County, Civil Action File No. 1:10-CV-4039-WSD (United States District Court for the Northern District of Georgia, Atlanta Division 2010).

Cooper, M. (2009). Aging Water Mains is Becoming Hard to Ignore. *The New York Times*. Retrieved from https://www.nytimes.com/2009/04/18/us/18water.html

De Bénédittis, J., & Bertrand-Krajewski, J. L. (2005). Infiltration In Sewer Systems: Comparison Of Measurement Methods. *Water Science and Technology, 52*(3), 219-227. doi:10.2166/wst.2005.0079

DeKalb County DWM. (2015a). *Ongoing Sewer Assessment Rehabilitation Program*. Retrieved from https://www.dekalbcountyga.gov/sites/default/files/OSARP.pdf

DeKalb County DWM. (2015b). System-Wide Flow And Rainfall Monitoring Program. *DeKalb County Department of Watershed Management (DWM) Capacity, Management, Operations, and Maintenance (CMOM) Program*, 44. Retrieved from https://www.dekalbcountyga.gov/sites/default/files/prog_updates_system_wide_flow_&_rainfall_monitoring_program.pdf

Diem, J., Hill, T. C., & Milligan, R.A. (2018). Diverse Multi-Decadal Changes In Streamflow Within A Rapidly Urbanizing Region. *Journal of Hydrology, 556*, 61-71. doi:10.1016/j.jhydrol.2017.10.026

Drinan, J.E., & Spellman, F.R. (2013). *Water and Wastewater Treatment: A Guide for the Nonengineering Professional* (Second ed.). Boca Raton, Florida: Taylor & Francis Group.

EPA. (2004). *Report to Congress: Impacts and Control of CSOs and SSOs*. Washington, D.C.: Office of Water. Retrieved from https://nepis.epa.gov/Exe/ZyPDF.cgi/30006O5F.PDF?Dockey=30006O5F.PDF

EPA. (2014). *Guide for Estimating Infiltration and Inflow*. Retrieved from https://www3.epa.gov/region1/sso/pdfs/Guide4EstimatingInfiltrationInflow.pdf

EPD. (2008). *Georgia Comprehensive State-wide Water Management Plan*. Atlanta, Georgia: State of Georgia. Retrieved from https://waterplanning.georgia.gov/sites/waterplanning.georgia.gov/files/related_files/water_plan_20080109.pdf

Ferguson, A. P., & Ashley, W. S. (2017). Spatiotemporal Analysis Of Residential Flood Exposure In The Atlanta, Georgia Metropolitan Area. *Natural Hazards, 87*, 989-1016. doi:10.1007/s11069-017-2806-6

Gillespie, D. M. (2016). “Revolutionize Life in the Chattahoochee River Valley": Buford Dam and the Development of Northeastern Georgia, 1950-1970. *Georgia Historical Quarterly, 100*(4), 404-440. Retrieved from https://search.ebscohost.com/login.aspx?direct=true&AuthType=ip,shib&db=a9h&AN=121213791&site=eds-live&scope=site&custid=gsu1

Gordon, D.W., & Painter, J.A. (2018). *Groundwater Conditions in Georgia, 2015-16*. Reston, Virginia: U.S. Geological Survey. doi:10.3133/sir20175142

Gwinnett County. (2020). Septic Tanks. Retrieved from https://www.gwinnettcounty.com/web/gwinnett/departments/water/geteducated/septictanks

Homer, C., Dewitz, J., Jin, S., Xian, G., Costello, C., Danielson, P., et al (2020). Conterminous United States Land Cover Change Patterns 2001–2016 From The 2016 National Land Cover Database. *ISPRS Journal of Photogrammetry and Remote Sensing, 162*, 184-199. doi:10.1016/j.isprsjprs.2020.02.019

Hyeon-Shik, B., Hyung Seok, J., & Abraham, D. M. (2006). Estimating Transition Probabilities in Markov Chain-Based Deterioration Models for Management of Wastewater Systems. *Journal of Water Resources Planning & Management, 132*(1), 15-24. doi:10.1061/(ASCE)0733-9496(2006)132:1(15)

Jacobson, C. R. (2011). Identification And Quantification Of The Hydrological Impacts Of Imperviousness In Urban Catchments: A Review. *Journal of Environmental Management, 92*(6), 1438-1448. doi:10.1016/j.jenvman.2011.01.018

Kaufman, D. R. (2007). *Peachtree Creek: A Natural and Unnatural History of Atlanta's Watershed*. Athens, Georgia: The University of Georgia Press.

Kerr Wood Leidal Associates. (2011). *Inflow and Infiltration Management Plan Template-Working Draft*. Burnaby, BC, Canada.

Kesik, T. (2015). *Best Practices Guide: Management Of Inflow And Infiltration In New Urban Developments*. Toronto, Ontario, Canada: Institute for Catastrophic Loss Recution.

King County. (2020). Infiltration and Inflow Sources in King County, Washington. King County Department of Natural Resources and Parks, Watewater Treatment Division. Retrieved from https://kingcounty.gov/services/environment/wastewater/ii.aspx

Klepper, D. (2015). Billions Needed to Fix New York's Aging Water Pipes. NBC New York. Retrieved from https://www.nbcnewyork.com/news/local/nyc-billions-needed-fix-states-cities-aging-water-pipes/1166392/

Lanning, A., Peterson, E.W. (2012). Evaluating Subdivisions for Identifying Extraneous Flow in Seperate Sanitary Sewer Systems. *Journal of Water Resource and Protection*. doi:http://dx.doi.org/10.4236/jwarp.2012.46037

McWillians, J. (2012). Atlanta's Sewers a Cautionary Tale, and a Heavy Bill. *Atlanta Journal Constiution.* Retrieved from https://www.ajc.com/news/local/atlanta-sewers-cautionary-tale-and-heavy-bill/otCOUgCKI85zN8rvX4SnoI/.

Mohrlok, U., Wolf, L., Kilnger, J. (2008). Quantification Of Infiltration Processes In Urban Areas By Accounting For Spatial Parameter Variability. *Journal of soils and sediments, 8*(1), 34-42.

Myeong, S., Nowak, D., Hopkins, P., & Brock, R. (2003). Urban Cover Mapping Using Digital, High-Spatial Resolution Aerial Imagery. *Urban Ecosystems, 5*, 243-256. doi:10.1023/A:1025687711588

Neighborhood Nexus. (2017) *DeKalb County Profile*. Retrieved from: https://neighborhoodnexus.org/maps-and-data/profiles/county-profiles/dekalb-county-profile/

Neumann, K., Lyons, W. B., Graham, E. Y., & Callender, E. (2005). Historical Backcasting Of Metal Concentrations In The Chattahoochee River, Georgia: Population Growth And Environmental Policy. *Applied Geochemistry, 20*(12), 2315-2324. doi:10.1016/j.apgeochem.2005.07.005

Oke, T., Mills, G., Christen, A., & Voogt, J. (2017). *Urban Climates*. Cambridge: Cambridge University Press. doi: 10.1017/9781139016476.009

Oszczapińska, K. (2020). Materials and Prices of Sewage and Water Systems in Poland. *Journal of Ecological Engineering, 21*(1), 34-39. doi:10.12911/22998993/113414

Paul, M., & Meyer, J. (2008). Streams in the Urban Landscape. In: Marzluff J.M. et al. (Eds) *Urban Ecology* (207-231). Springer, Boston, MA. doi:10.1007/978-0-387-73412-5_12

Peters, N. E. (2009). Effects Of Urbanization On Stream Water Quality In The City Of Atlanta, GA. *Hydrologic Processes, 23*, 2860-2878. doi:10.1002/hyp.7373

Peters, N. E., & Aulenbach, B. T. (2011). Water Storage At The Panola Mountain Research Watershed, Georgia, USA. *Hydrological Processes, 25*(25), 3878-3889. doi:10.1002/hyp.8334

Rodel, S., Gunthert, F.W., & Buggemann, T. (2017). Investigating The Impacts Of Extraneous Water On Wastewater Treatment Plants. *Water Science & Technology*, *75*(4), 847-855. doi:10.2166/wst.2016.570

Rose, S., & Peters, N. E. (2001). Effects Of Urbanization On Streamflow In The Atlanta Area (Georgia, USA): A Comparative Hydrological Approach. *Hydrological Processes, 15*(8), 1441-1457. doi:10.1002/hyp.218

Seager, R., Tzanova, A., & Nakamura, J. (2009). Drought in the Southeastern United States: Causes, Variability over the Last Millennium, and the Potential for Future Hydroclimate Change. *Journal of Climate, 22*(19), 5021-5045. doi:10.1175/2009jcli2683.1

Smucygz, B., Clayton, J. A., & Comarova, Z. (2010). Comparison of Changes in Runoff and Channel Cross-sectional Area as a Consequence of Urbanization for Three Chattahoochee River Subbasins, Georgia, USA. *Southeastern Geographer, 50*(4), 468. doi:10.1353/sgo.2010.0005

Stamer, J.K., Cherry, R.N., Faye, R.E., & Kleckner, R.L. (1976). Magnitudes, Nature, Effects of Point and Nonpoint Discharges in the Chattahoochee River Basin, Atlanta to West Point Dam, Georgia. Geological Survey Water-Supply Paper 2059. Retrieved from https://pubs.usgs.gov/wsp/2059/report.pdf

Staufer, P., Scheidegger, A., & Rieckermann, J. (2012). Assessing The Performance Of Sewer Rehabilitation On The Reduction Of Infiltration And Inflow. *Water Research, 46*(16), 5185-5196. doi:10.1016/j.watres.2012.07.001

Thapa, J. B., Jung, J. K., & Yovichin, R. D. (2019). A Qualitative Approach to Determine the Areas of Highest Inflow and Infiltration in Underground Infrastructure for Urban Area. *Advances in Civil Engineering, 2019*, 1-11. doi:10.1155/2019/2620459

U.S. Census Bureau. (2019). *QuickFacts DeKalb County, Georgia*. Retrieved from: https://www.census.gov/quickfacts/dekalbcountygeorgia

Walsh, C. J., Fletcher, T., & Ladson, T. (2005). Stream Restoration In Urban Catchments Through Redesigning Stormwater Systems: Looking To The Catchment To Save The Stream. *Journal of The North American Benthological Society - J N AMER BENTHOL SOC*, *24*(3), 690-705. doi:10.1899/0887-3593(2005)024\[0690:SRIUCT\]2.0.CO;2

Wittenberg, H., & Aksoy, H. (2010). Groundwater Intrusion Into Leaky Sewer Systems. *Water Science & Technology- WST*, *62*(1), 92-98. doi:10.2166/wst.2010.287

WPA (1936). Works Progress Administration in Georgia Photographs In *Atlanta Connally Sewer, 11/31/1936*. Manuscript 996. Hargrett Rare Book and Manuscript Library, The University of Georgia Libraries. Retrieved from http://hmfa.libs.uga.edu/hmfa/view?docId=ead/ms996-ead.xml

Zhang, Z. (2005). Flow Data, Inflow/Infiltration Ratio, and Autoregressive Error Models. *Journal of Environmental Engineering 131*(3), 343-349. doi:10.1061/(ASCE)0733-9372(2005)131:3(343)

Zhang, Z. (2007). Estimating Rain Derived Inflow and Infiltration for Rainfalls of Varying Characteristics. *Journal of Hydraulic Engineering, 133*(1), 98-105. doi:10.1061/(asce)0733-9429(2007)133:1(98)